UNIVERSITÄT
BERN

Faculty of Business, Economics
and Social Sciences

Department of Economics

**World GDP, Anthropogenic Emissions,
and Global Temperatures, Sea Level, and Ice Cover**

Luca Benati

25-03

March, 2025

DISCUSSION PAPERS

Schanzeneckstrasse 1
CH-3012 Bern, Switzerland
http://www.vwi.unibe.ch

World GDP, Anthropogenic Emissions, and Global Temperatures, Sea Level, and Ice Cover*

Luca Benati
University of Bern†

Abstract

I use Bayesian VARs with stochastic volatility to forecast global temperatures and sea level and ice cover in the Northern emisphere until 2100, by exploiting (*i*) their long-run equilibrium relationship with climate change drivers (CCDs) and (*ii*) the relationship between world GDP and anthropogenic CCDs. Assuming that trend GDP growth will remain unchanged after 2024, and the world economy will fully decarbonize by 2050, global temperatures and the sea level are projected to increase by 2.3 Celsius degrees and 38 centimeters respectively compared to pre-industrial times. Further, uncertainty is substantial, pointing to significant upward risks. Because of this, bringing climate change under control will require a massive programme of carbon removal from the atmosphere, in order to bring anthropogenic CCDs back to the levels of the end of the XX century.
Keywords: Climate change; Bayesian VARs; stochastic volatility; cointegration; forecasting; conditional forecasts.
JEL Classification: E2, E3.

*A previous version of this work was presented under a different title ('Forecasting Global Temperatures by Exploiting Cointegration with Radiative Forcing') at the IWEEE 2024 and ESOBE 2024 meetings, the 2024 workshop 'Energy Transition and Climate Change' at the University of California Riverside, the Second International Conference on the Climate-Macro-Finance Interface at Bayes Business School, and a seminar at Banca d'Italia. I wish to thanks participants, as well as Jennifer Castle, Giuseppe Cavaliere, Jesus Gonzalo, David Hendry, Lutz Kilian, Helmut Luetkepohl, and Bill McGuire, for useful discussions, suggestions and/or comments. Special thanks to Jonathan Wright for very useful suggestions on testing for the null of cointegration with I(2) data, and to Marco Del Negro for extremely useful suggestions across the board. Usual disclaimers apply. All of the data and the computer programs (written in MATLAB) are available upon request.

†Department of Economics, University of Bern, Schanzeneckstrasse 1, CH-3001, Bern, Switzerland. Email: luca.benati@vwi.unibe.ch

1 Introduction

For more than a decade global temperatures have been consistently breaking records nearly every year. Against this background, the scorching summers of 2022, 2023 and 2024, characterized by heatwaves, droughts, wildfires and floods of an unprecedented spread and intensity, have highligthed in the starkest possible way the severity of the threat posed by climate change.

In this paper I use Bayesian VARs with stochastic volatility in order to forecast global temperatures and sea level and ice cover in the Northern emisphere until the end of the XXI century, by exploiting

(*i*) the relationship between world GDP and anthropogenic drivers of climate change (CO2, methane, clorofluorocarbons, sulphur emissions, ...);

(*ii*) the long-run equilibrium relationship between temperatures and either sea level or ice cover; and

(*iii*) the long-run equilibrium relationship between temperatures and all climate change drivers (CCDs) jointly considered, both anthropogenic and non-anthropogenic (i.e., volcanic activity and solar irradiance). Such long-run relationship is a key tenet of climate science, and it is in fact an implication of physics laws that can be (and it has been) tested within a laboratory setting under controlled conditions.

In line with the climate science literature, the literature on the econometrics of climate change, and the Intergovernmental Panel on Climate Change (IPCC) reports, I summarize the *joint* impact on temperatures of *all* CCDs via a single index, their so-called Joint Radiative Forcing (JRF). Intuitively, the radiative forcing of individual CCDs provides a quantitative measure, based on formulas from physics, of their ability to *trap heat* in the atmosphere. The JRF index provides therefore a quantitative summary of the *overall* ability of all CCDs *jointly considered* to trap heat. Because of this the JRF index is, in fact, *all that matters* as far as climate change is concerned. Permanent increases (decreases) in the JRF cause subsequent corresponding increases (decreases) in global temperatures.

I estimate VARs for world GDP, global temperatures, the sea level, ice cover in the Northern emisphere, anthropogenic radiative forcing (RF), and the radiative forcings of volcanic activity and solar irradiance. I impose

(1) *exogeneity* of both volcanic activity and solar irradiance with respect to the rest of the system;

(2) in line with a vast literature, *cointegration* between the JRF index and global temperatures;

(3) *cointegration* between global temperatures and either sea level or ice cover, a feature of the data that is very strongly supported by cointegration tests; and

(4) a *time-varying relationship* between world real GDP and anthropogenic RF (i.e., the 'carbon intensity' of GDP). As I discuss below, both conceptual reasons, and overwhelming empirical evidence, support the notion that the relationship has indeed materially evolved since the mid-XIX century.

Finally,

(5) I allow for *time-variation* in trend world real GDP growth, a feature of the data that is overwhelmingly supported by Stock and Watson's (1996, 1998) tests.

My goal is to provide tentative answers to the following questions: What are the increases in temperatures and the sea level, and the decrease in ice cover, that are *already implied* by the levels of CCDs reached in 2024? How will these variables evolve going forward under alternative scenarios for the dynamics of world GDP and its carbon intensity? And what are the reductions in CCDs that will be required in order to bring climate change under control?

1.1 Main results

Under an extreme scenario in which the state of the system is 'frozen' at 2024—with both the level of world GDP and its carbon intensity fixed at their 2024 values—median forecasts predict global temperatures to increase by nearly 5 Celsius degrees by 2100 compared to pre-industrial times, and the sea level to increase by 48 centimeters. In order to put these numbers into perspective it is worth recalling that 5 Celsius degrees is the lower bound of the estimates for the increase in temperatures associated with the so-called Paleocene-Eocene Thermal Maximum (PETM), about 55.5 million years ago. During that period Antarctica was covered with tropical forests, and Arctic waters pullulated with alligators. If temperatures were to increase by 5 degrees compared to pre-industrial times within less than eight decades, the extent to which society could adapt—or whether it could adapt at all—is entirely open to question. Quite simply, this would be a *different planet*, far removed from the range of temperatures under which human civilizations have flourished over the last 12 to 15 thousand years.

Under an alternative scenario in which trend GDP growth remains unchanged after 2024, and the world economy fully decarbonizes by 2050, median forecasts project temperatures and the sea level to increase by 2.3 degrees and 38 centimeters compared to pre-industrial times. Further, uncertainty is substantial, thus pointing to significant upward risks: e.g., the 90%-coverage credible set for temperatures stretches from 1.2 to 3.4 Celsius degrees. Alternative scenarios based on the same assumption for trend GDP growth and a slower pace of decarbonization, with zero carbon intensity reached in either 2075 or 2100, paint a significantly grimmer picture.

Evidence also shows that a decrease in economic growth, with trend real GDP growth falling by 1% either in 2025, or at several alternative future dates, does not materially change the overall picture, with temperatures still projected to increase by several Celsius degrees by 2100 compared to pre-industrial times. This shows that the possible future deceleration of economic growth (due e.g. to the ongoing fall in population growth) will only marginally affect climate change. The implication is that full decarbonization of GDP is the only possible solution.

Under this respect, evidence shows that, even if we were somehow able to 'freeze'

JRF at its 2024 level, the intrinsic dynamics of the system will *necessarily* imply substantial increases in temperatures going forward: e.g., about two-thirds of the density of the forecast of temperatures for 2100 is above the benchmark of the Paris climate agreements, with a median projection equal to 1.7 degrees, and the upper limit of the 90 per cent-coverage credible set equal to 2.2 degrees. It is important to stress that these increases were already 'locked in' by 2024, which implies that CCDs have *already exceeded* the levels climate scientists regard as dangerous. The implication is that, in order to exit the danger zone, CCDs will have to be *brought back* to the levels that had prevailed sometimes before 2024. The obvious question is 'By how much?'. Under this respect, forecasts conditional on alternative paths for CCDs show that, given the extent of statistical uncertainty, exiting the danger zone will require bringing CCDs back to the levels of the end of the XX century.

Until the 1970s, the accumulation in the atmosphere of anthropogenic sulphur emissions as a by-product of burning fossil fuels had blocked solar radiation to a significant extent, thus *mitigating* the temperature increases caused by other CCDs. This is what James Hansen has labelled as the 'Faustian bargain' our civilization has been entertaining for two centuries. Since then, the progressive removal of sulphur from the atmosphere has caused the process to go into *reverse*. As a result, since the early 1980s the evolution of the accumulated stock of sulphur emissions has contributed to an *increase* in global temperatures. Evidence suggests that even if we were somehow able to keep the other CCDs fixed at the level they reached in 2024, the complete removal of anthropogenic sulphur emissions from the atmosphere, *by itself*, would cause sizeable increases in temperatures going forward.

The paper is organized as follows. The next section discusses the data, whereas Section 3 discusses statistical evidence on their stochastic properties. Section 4 discusses my econometric approach, and Section 5 discusses the evidence: impulse-response functions to a permanent shock to the JRF index; and forecasts up to the end of the XXI century, both unconditional, and conditional on alternative possible paths for the evolution of the world GDP. Section 7 concludes.

2 The Data

Online Appendix A describes in detail the data and their sources, which are both standard in the literatures on climate science and the econometrics of climate change.

I consider nine drivers of climate change: CO2, methane (CH4), nitrous oxide (N2O), chlorofluorocarbons (CFC11 and CFC12), anthropogenic sulfur emissions (SOx), El Niño and La Niña (El Niño-Southern Oscillation, henceforth ENSO), solar irradiance, and volcanic activity. In line with the literature, I convert each individual CCD into radiative forcing (RF, expressed in Watts per square meter) based on standard formulas from physics (see Online Appendix A). Once each CCD has been converted into RF, I construct the *aggregate* JRF index as in Kaufmann, Kauppi, and Stock (2006) by summing up the individual components. As shown by Kaufmann,

Kauppi, and Stock (2006, see Table II and the discussion on page 261), it is indeed not possible to reject the null hypothesis that 'the temperature effect of a unit of radiative forcing (e.g. W/m^2) is equal across forcings'. The single exception is ENSO, which I ignore for the reasons I discuss in Online Appendix A.4.[1] By the same token, I construct a corresponding index of *anthropogenic* RF, defined as the sum of the RFs of CO2, CH4, N2O, CFC11, CFC12, and SOx.

I consider an index of global[2] temperatures (in Celsius degrees) for the entire planet. As it is routine in the literature, temperatures are expressed as 'anomalies', i.e. as *deviations* from a benchmark value. Following standard practice (see e.g. the IPCC reports) I take the average temperature over the period 1850-1900 as the benchmark, so that the temperature anomaly I work with is computed as deviation from such benchmark.

Finally, I consider a series for world real GDP, an index of ice cover in the Northern emisphere (in squared kilometers), and an index for the world sea level (in centimeters).

The sample period is 1850-2024.

2.1 A look at the raw data

Figure 1 shows the radiative forcing of individual climate change drivers; the JRF index minus volcanic RF, either including or excluding the radiative forcing of anthropogenic sulfur emissions (SOx); the global temperature anomaly, the world sea level, and the index of ice cover in the Northern emisphere; and either the logarithm or the growth rate of world real GDP.

Starting from the radiative forcing of the particulates injected by volcanic activity into the atmosphere, three main findings emerge from the first panel of Figure 1. First, volcanic RF is uniformly *negative*. This is because the dust spewn into the atmosphere by volcanoes prevents a fraction of solar radiation from reaching Earth in the first place, so that its impact on JRF is by definition negative. Second, volcanic RF is extraordinarily volatile, and it is manifestly characterized by a sizeable extent of heteroskedasticity. Third, although over very long periods of time[3] volcanic activity—and therefore volcanic RF—does not exhibit any trend, over comparatively short periods (such as the sample I am here working with) there are sometimes transitory shifts in the mean, due to temporary increases in volcanic activity. This is the case within the present context. A Bai and Perron (1998, 2003) test for multiple breaks at unknown points in the sample in the mean of the series plotted in the first

[1] In brief, ENSO features virtually no spectral power at frequencies beyond 25 years, and it is extraordinarily noisy compared to the other drivers of climate change. The implication is that including the radiative forcing of ENSO in the JRF index would uniquely add a large amount of high-frequency noise, whereas it would bring essentially *no information* about the long-horizon developments that are the focus of the present work.

[2] I,.e., for the whole planet.

[3] The index of volcanic activity I am working with starts in the year 1500.

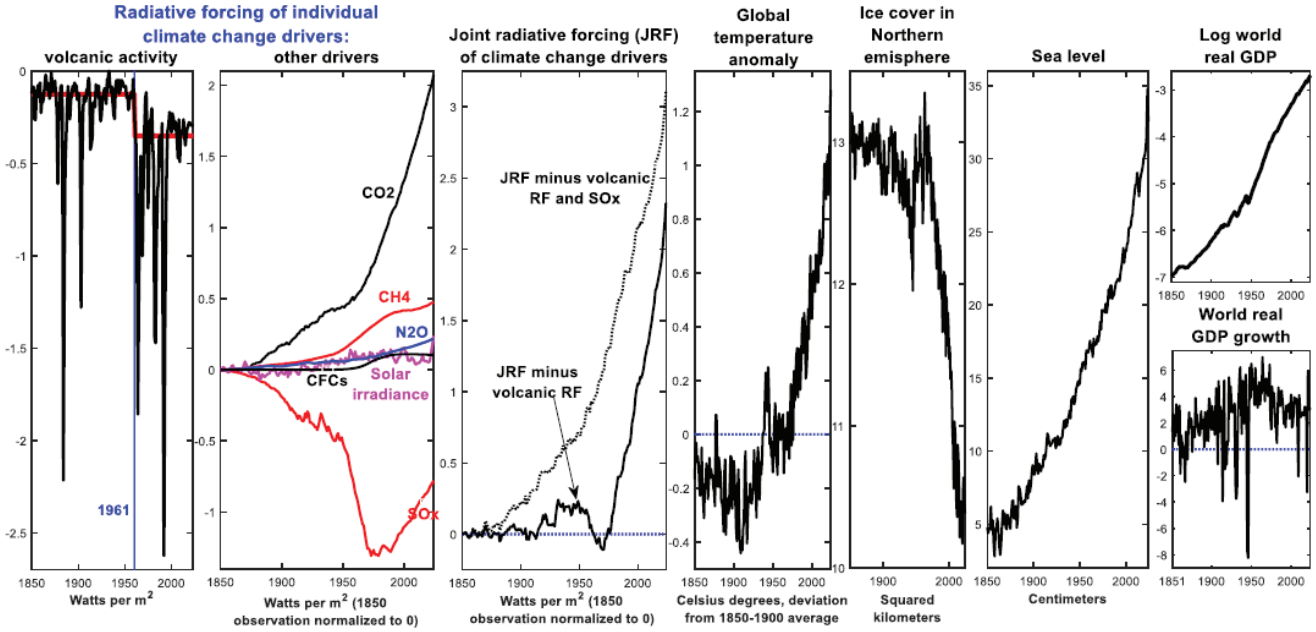

Figure 1 The raw data

panel of Figure 1, bootstrapped as in Diebold and Chen (1996), detects a break in 1961, with the p-values for the UD_{Max} and WD_{Max} test statistics equal to 0.050 and 0.056 respectively,[4] and the medians for the two sub-samples being equal to -0.126 and -0.351 respectively.[5] Although volcanic RF is stationary,[6] and therefore provides *no contribution* to the secular increase in JRF, this evidence illustrates why it is important to take it into account in the empirical work. First, the downward shift in the series since 1961 has had a *negative* impact on the overall JRF index, thus counteracting the impact of increases in other CCDs, and causing therefore temperatures to increase by *less* than they would otherwise. Not including volcanic RF in the model would therefore distort the evidence. In particular, since hundreds of years of data on volcanic emissions suggest that the post-1961 shift will ultimately disappear—so that the RF of other CCDs will ultimately fully reveal itself—ignoring volcanic RF would introduce a downward distortion in temperatures' forecasts. Second, the series' large volatility compared to other CCDs, together with its heteroskedasticity, suggests once again that ignoring it would likely distort the inference. In Section 4 I will discuss in detail how I model both the heteroskedasticity (via stochastic volatility) and the shift in the mean in 1961.

Turning to the other drivers of climate change, and to the aggregate indices of radiative forcing, two main findings emerge from the second and third panels of Figure 1. First, since 1850 CO2, CH4 and SOx have been by far the dominant drivers of the evolution of the JRF index. Second, until about the 1970s SOx had been playing an important moderating role in the overall increase in the JRF index. Since then, however, its previous moderating contribution has gone into reverse, as efforts to remove anthropogenic sulfur emissions from the atmosphere have started to bear fruits. As a result, over the last three decades the evolution of SOx's radiative forcing has contributed to the overall increase in the JRF index.

The third panel of Figure 1 illustrates this point in an especially stark way. Normalizing the two indices[7] to zero in 1850, excluding the impact of SOx the index would have increased much faster than it has historically been the case. To the extent that efforts to remove anthropogenic sulfur emissions from the atmosphere will continue and will be successful, the radiative forcing of SOx shown in the second panel will converge to zero, and the overall JRF index will therefore be more and more dominated by the remaining drivers. The implications of this are sobering. As

[4] On the other hand, the $F_T(2|1)$ test does not detect a second break in the mean, with the bootstrapped p-value equal to 0.1496.

[5] Throughout the entire paper I focus on the medians of the two sub-samples, rather than the means, because of the significant extent of heteroskedasticity.of volcanic RF.

[6] As discussed in Section B.1 in the Online Appendix, Elliot et al.'s (1996) tests strongly reject the null of a unit root in the series, either controlling or not controlling for the identified break in the mean.

[7] We exclude from both indices volcanic RF (i.e., the series plotted in the first panel), because its large volatility compared to other RF series would make the two indices very noisy. This is without any loss of generality, since volcanic activity is stationary.

shown in the third panel, if in 2024 we had somehow been able to remove SOx from the atmosphere, the normalized JRF excluding volcanic RF would have shot up from about 2.7 to 3.2. The implication is stark. Even if we were able to keep the non-SOx radiative forcing fixed at the level reached in 2024, efforts to clean up the atmosphere of SOx, *by themselves*, automatically imply sizeable increases in temperatures going forward.

A similar point holds for volcanic eruptions. As previously mentioned, although over very long periods of time the amount of particulates injected into the atmosphere by volcanic eruptions does not show any trend, in a few instances—such as over the period since 1961—it exhibits a clear shift in the mean. Exactly as for SOx, the fact that since the early 1960s volcanic RF has been *more negative* than it had been before implies that, to the extent that the pre-1961 pattern of eruptions will ultimately reassert itself, global temperatures will *necessarily* increase by non-negligible amounts even in the absence of any change in the other drivers of radiative forcing. In particular, if the median volcanic RF were to revert back to its pre-1961 value of -0.126, in Europe temperatures would increase by 0.22 Celsius degrees.[8]

This, together with the previous discussion about the impact of cleaning up the atmosphere of SOx, shows that even without further increases in the drivers of climate change, there is already, deeply embedded in the system-Earth, a sizeable amount of *committed warming*, i.e. future temperature increases that are already 'baked in the cake' and impossible to avoid other than by removing carbon from the atmosphere, geoengineering, etc. As we will see in Section 5.4, due to the comparatively long lags with which global temperatures increase following an increase in radiative forcing, there is in fact additional committed warming already embedded in the system-Earth.

The fourth, fifth, and sixth panels provide a stark illustration of the main features of the global heating phenomenon, with dramatic increases in temperatures and the sea level since 1850, and a marked shrinkage of the ice surface in the Northern emisphere. Further, the phenomenon has clearly accelerated over the most recent decades. This is especially clear for temperatures and ice cover, and less so for the sea level (as I discuss below, in the long run the sea level approximately evolves with the cubic root of global temperatures).

Finally, the last two panels, especially the bottom one, highlight sizeable changes in the growth rate of world real GDP since 1850, with average growth first progressively increasing up until the 1960s-1970s, then decreasing, and finally seemingly stabilizing at about 2-3 per cent.

2.2 The long-run equilibrium relationships

Figure 2 illustrates the long-run equilibrium (i.e., as we will see, *cointegration*) relationships that are embedded in the system. The first panel shows the relationship

[8] This is because the cointegration vector between the temperature anomaly for the European continent and the JRF index is indistinguishable from $[1\ -1]'$. This evidence is available upon request.

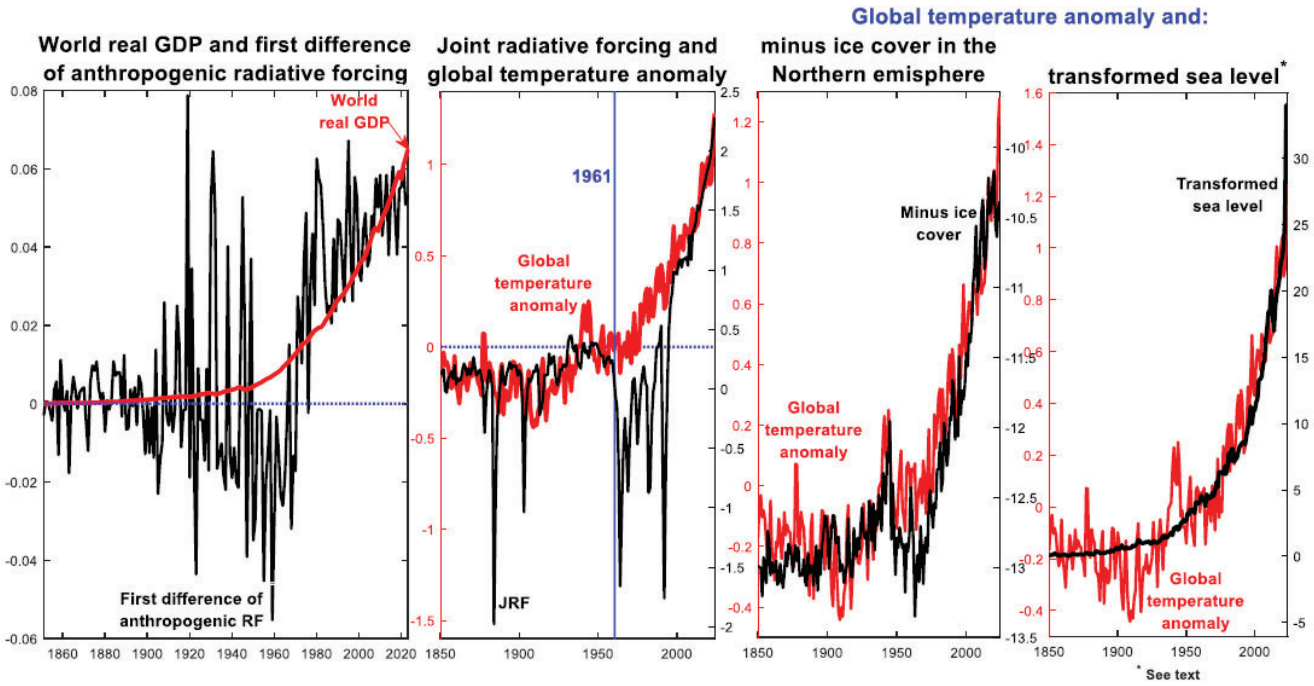

Figure 2 The long-run equilibrium relationships

between the *level* (not the logarithm) of world real GDP and the *first difference* of anthropogenic RF, which as discussed in Section 2 is defined as the sum of the RFs pertaining to CO2, CH4, N2O, CFC11, CFC12, and SOx. The reason why the long-run relationship pertains to the level of the former series and the first difference of the latter is straightforward. Every year, in order to produce a certain amount of real output, the world economy uses a corresponding amount of energy. This translates into corresponding *new emissions* of CO2, CH4, etc., which add to the *existing stocks* of anthropogenic CCDs.[9] In turn, this leads to a progressive increase, year after year, in the level of anthropogenic RF, which is the fundamental driver of climate change. The implication is that, both as a matter of logic, and in practice, the relationship pertains to the level of world real GDP, and the change in (i.e. the first difference of) the anthropogenic RF index.

Two things are apparent from the first panel of Figure 2. First, in the long-run the two series tend indeed to closely co-move. Second, in the short-to-medium run they tend however to deviate from each other. Although most of these deviations are quite short-lived, and they can therefore be thought of as 'noise' contaminating the fundamental relationship determined by the 'carbon intensity' of GDP, the period between the 1930s and the end of the 1970s clearly appears different from the rest of the sample, with a persistent *negative* change in anthropogenic RF. As it is apparent from the second panel of Figure 1, this was caused by a dramatic increase in the amount of SOx during that period. Then, starting from the 1970s, SOx first peaked, and then started being removed from the atmosphere, with the result that the positive relationship between world real GDP and the first difference of anthropogenic RF reasserted itself. In Section B.3 in the Online Appendix I show that the two series are indeed cointegrated.

The second panel of Figure 2 shows the long-run relationship between the JRF index and the global temperature anomaly. The long-run equilibrium relationship between the series is quite clearly apparent. Notice that the previously discussed downward shift in the mean of volcanic RF in 1961 caused a temporary divergence between the JRF index and temperatures. However, since volcanic RF, although subject to infrequent and temporary shifts in the mean, is stationary, the long-run relationship between the two series ultimately reasserted itself. Again, in Section B.3 in the Online Appendix I show that the JRF is indeed cointegrated with temperature anomalies.

The third panel shows the long-run relationship between global temperatures and *minus* the ice cover in the Northern emisphere. The figure speaks for itself, and it clearly points towards cointegration between the two series, a feature of the data that is strongly supported by statistical tests.

[9] To be precise, each CCD has a certain *half-life* in the atmosphere. E.g. the half-life of CO2 is about 120 years, whereas that of methane is about 10.5 years. The fact that the dominant CCD, CO2, has such a long half-life implies that although strictly speaking shocks to anthropogenic RF are ultimately transitory, for practical purposes they can be regarded as permanent.

Finally, the last panel shows shows the long-run relationship between global temperatures and a *non-linear transformation* of the sea level series. Evidence indeed quite clearly suggests that, in the long run, the sea level approximately evolves with the cubic root of global temperatures. In particular, the best fit is provided by an exponent equal to 2.94, rather than exactly 3. The transformed sea level series plotted in the last panel of Figure 2 is therefore equal to the 'raw' sea level series raised to the power of 2.94. Again, the evidence speaks for itself, and it strongly suggests that in the long run the two series in the panel, once appropriately rescaled, move one-for-one.

3 Stochastic Properties of the Data

Online Appendix B features an extensive analysis of the stochastic properties of world GDP and climate change series, based on unit root and cointegration tests; tests for breaks in the mean; and Stock and Watson's (1996, 1998) tests of the null of time-invariance in the Data Generation Process (DGP) for the first differences[10] of individual series, against the alternative of random-walk time-variation in the mean. Overall, evidence strongly and consistently suggests that

(1) in line with the evidence in Figure 1, trend world real GDP growth has exhibited a significant extent of time-variation over the sample period.

(2) Solar irradiance has evolved essentially as a random-walk with drift, reflecting its well-known long-run secular increase, whereas volcanic RF has been very strongly stationary, either controlling or not controlling for the identified break in the mean. Except for volcanic RF's heteroskedasticity, there is no evidence of time-variation in the stochastic properties of either series.

(3) Temperature anomalies, the transformed sea level, the ice cover series, and anthropogenic RF are all I(2). In particular, their first differences feature a random-walk component that is very strongly and uniformly detected across the board by Stock and Watson's (1996, 1998) tests.

(4) In line with previous cointegration-based studies of climate change, the levels of the JRF index and of temperature anomalies are cointegrated. As mentioned, this is in fact what physics predicts it should be. By the same token, the level of world GDP is cointegrated with the first difference of anthropogenic radiatiave forcing.

(5) Global temperatures are cointegrated with either ice cover, or the transformed sea level series.

Since evidence is near-uniformly very strong and consistent, in this section I do not discuss it in detail. The interested reader is referred to Online Appendix B for a detailed discussion of both technical details, and the evidence itself.

Intuitively, the reason for the presence of time-variation in the means of the first differences of the temperature anomaly, sea level, ice cover, and anthropogenic RF is

[10] Since volcanic RF is I(0), for this series I consider the level.

straightforward. The system-Earth went from a period, before the Industrial Revolution, characterized by virtually no economic growth—and therefore negligible emissions of anthropogenic CCDs—to the subsequent period characterized by the progressive spreading of economic growth across the globe. As an increasing number of countries experienced sustained growth, their emissions of CCDs increased accordingly. The consequence of this is the progressive *long-term acceleration* in the rate of overall increase of CCDs. A second main reason for such acceleration is the fact that, as mentioned, until the 1970s the accumulation of anthropogenic sulphur emissions in the atmosphere partly mitigated the impact of increases in the other CCDs. Since then, however, the progressive removal of sulphur has thrown this process into reverse. This implies that the rate of change of the *joint* impact of all CCDs, as captured by the JRF index, has exhibited a non-negligible extent of variation over the sample period.

I now turn to discussing my econometric approach.

4 The Econometric Approach

4.1 The benchmark model

4.1.1 Exogenous drivers of climate change

World real GDP Based on the evidence from Stock and Watson's (1996, 1998) tests reported in Section B.2 in the Online Appendix, I assume that the time-varying mean of the log-difference of world real GDP, μ_t, evolves as a random walk:

$$\mu_t = \mu_t + \epsilon_t^{\mu}, \tag{1}$$

with $\epsilon_t^{\mu} \sim N(0,\ \sigma_{\mu}^2)$. The deviation from μ_t of the log-difference of GDP, $\Delta y_t = \Delta \ln GDP_t$, is then postulated to evolve as an AR(p) process,

$$\Delta y_t - \mu_t = \phi_1(\Delta y_{t-1} - \mu_{t-1}) + ... + \phi_p(\Delta y_{t-p} - \mu_{t-p}) + \epsilon_t^{\Delta y} \tag{2}$$

with $\epsilon_t^{\Delta y} \sim N(0,\ \sigma_{\Delta y,t}^2)$, where $\sigma_{\Delta y,t}^2$ is a time-varying variance which, as I discuss below, is postulated to evolve according a stochastic volatility specification.

Volcanic radiative forcing Based on the evidence from Elliot et al.'s (1996, 1998) and Stock and Watson's (1996, 1998) tests reported in Section B.2 in the Online Appendix, I assume that the deviation from its mean of the *level* of volcanic RF, RF_t^V, follows an AR(p) process,

$$RF_t^V - \delta_t = \psi_1(RF_{t-1}^V - \delta_{t-1}) + ... + \psi_p(RF_{t-p}^V - \delta_{t-p}) + \epsilon_t^V \tag{3}$$

with δ_t equal to either δ_1, before 1961, or δ_2, after that, and with $\epsilon_t^V \sim N(0,\ \sigma_{V,t}^2)$, with $\sigma_{V,t}^2$ being a time-varying variance.

Solar radiative forcing By the same token, I assume that the *first difference* of solar RF, ΔRF_t^S, also follows an AR(p) process,

$$\Delta RF_t^S - \xi = \varphi_1(\Delta RF_{t-1}^S - \xi) + ... + \varphi_p(\Delta RF_{t-p}^S - \xi) + \epsilon_t^S \tag{4}$$

with $\epsilon_t^S \sim N(0,\, \sigma_{S,t}^2)$.

4.1.2 Long-run equilibrium relationships

Based on the evidence from Wright's (2000) tests reported in Section B.3 in the Online Appendix, I assume that the level of the global temperature anomaly is cointegrated with the level of the JRF index, so that in a long-run equilibrium

$$JRF = \alpha T \tag{5}$$

where JRF is the JRF index, T is either the temperature anomaly, and α is the cointegration coefficient.

I also assume that in a long-run equilibrium the change in anthropogenic RF, ΔRF_t^A, is a function of the level (not the logarithm) of world GDP, GDP_t, through a coefficient of 'anthropogenic RF intensity' (or 'carbon intensity', as a shorthand) of GDP, β_t,

$$\Delta RF_t^A = \beta_t GDP_t \tag{6}$$

In line with the discussion in Section 2.1, I assume that β_t evolves as a random walk,

$$\beta_t = \beta_t + \epsilon_t^\beta, \tag{7}$$

with $\epsilon_t^\beta \sim N(0,\, \sigma_\beta^2)$. The rationale for this specification is the following. Anthropogenic RF is defined as the sum of the radiative forcing of CO2, methane, nitrous oxide, chlorofluorocarbons, and anthropogenic sulphur emissions. Due to technological progress, since 1850 the amount of anthropogenic CCDs emitted for one unit of world GDP has changed quite significantly. E.g., in the XIX century energy was produced mainly by burning carbon, whereas in the XX century the world economy mostly switched to oil, and in recent years partly to renewables. Further, as discussed, the progressive cleaning up of the atmosphere from sulphur emissions since the 1970s has injected a further element of time-variation in the relationship between GDP and anthropogenic RF.

Finally, in line with the evidence in the last two panels of Figure 2, I assume that the global temperature anomaly is cointegrated with either minus the ice cover, or the transformed sea level series, so that in a long-run equilibrium

$$T = \gamma_S S = \gamma_I I \tag{8}$$

where S and I are the the transformed sea level and ice cover series, and γ_S and γ_I are their respective cointegration coefficients.

4.1.3 The structural VAR representation

I assume that conditional on the paths of the exogenous processes—μ_t, Δy_t, RF_t^V, ΔRF_t^S, and β_t—the evolution of the system is fully characterized by a *structural VAR* (SVAR) representation for

(1) the cointegration residual between the JRF index and the global temperature anomaly;

(2) the cointegration residuals between the temperature anomaly and either ice cover or the transformed sea level index; and

(3) the deviation of the change in anthropogenic RF from its equilibrium with world GDP implied by (6).

Assuming, for illustrative purposes, a SVAR with one lag, the dynamics of the system is characterized by

$$\underbrace{\begin{bmatrix} \Delta y_t - \mu_t \\ \Delta RF_t^A - \beta_t GDP_t \\ JRF_t - \alpha T_t \\ T_t - \gamma_I I_t \\ T_t - \gamma_S S_t \\ RF_t^V - \delta_t \\ \Delta RF_t^S - \xi \end{bmatrix}}_{Y_t} = \underbrace{\begin{bmatrix} x & & & & & & \\ x & x & x & x & x & & \\ x & x & x & x & x & x & x \\ x & x & x & x & x & x & x \\ x & x & x & x & x & x & x \\ & & & & & x & \\ & & & & & & x \end{bmatrix}}_{B_1} \underbrace{\begin{bmatrix} \Delta y_{t-1} - \mu_{t-1} \\ \Delta RF_{t-1}^A - \beta_{t-1} GDP_{t-1} \\ JRF_{t-1} - \alpha T_{t-1} \\ T_{t-1} - \gamma_I I_{t-1} \\ T_{t-1} - \gamma_S S_{t-1} \\ RF_{t-1}^V - \delta_{t-1} \\ \Delta RF_{t-1}^S - \xi \end{bmatrix}}_{Y_{t-1}} +$$

$$+ \underbrace{\begin{bmatrix} 1 & & & & & & \\ + & 1 & & & & & \\ + & + & 1 & & & + & + \\ + & + & x & 1 & & + & + \\ + & + & x & x & 1 & + & + \\ & & & & & 1 & \\ & & & & & & 1 \end{bmatrix}}_{A_0} \underbrace{\begin{bmatrix} \epsilon_t^{\Delta y} \\ \epsilon_t^A \\ \epsilon_t^{TSI} \\ \epsilon_t^{SI} \\ \epsilon_t^S \\ \epsilon_t^V \\ \epsilon_t^S \end{bmatrix}}_{\epsilon_t} \tag{9}$$

where A_0 is the impact matrix of the structural shocks; '+' labels a non-negative scalar; 'x' is a non-0 scalar on which no sign restriction is imposed; and all entries in either B_1 or A_0 that are not labelled as '1', '+', or 'x' are equal to 0. ϵ_t^A is a shock capturing variation in anthropogenic radiative forcing over and above that due to changes in the level of world real GDP. As such, it captures a wide range of phenomena, the most important of which is a sizeable portion of the secular variation in the stock of anthropogenic sulfur emissions. When SOx is removed from the atmosphere anthropogenic RF increases, whereas the impact on world real GDP is negligible to *nil*. ϵ_t^{TSI}, ϵ_t^{SI}, and ϵ_t^I are three orthogonalized shocks that do not have any specific interpretation. On impact ϵ_t^{TSI} only affects temperatures, ice cover, and the sea level; ϵ_t^{SI} only affects ice cover and the sea level; and ϵ_t^S only affects the sea level. Since neither shock has any clear interpretation, in what follows I will ignore them.

The matrices B_1 and A_0 encode the exogenous evolution of $\Delta y_t - \mu_t$, $RF_t^V - \delta_t$ and $\Delta RF_t^S - \xi$, each one uniquely as a function of its own lags and its own shocks. Further, B_1 assumes that the deviation of anthropogenic RF from its technology-dictated long-run equilbrium, $\Delta RF_t^A - \beta_t GDP_t$, is not affected by either volcanic or solar RF. The rationale for this is that $\Delta RF_t^A - \beta_t GDP_t$ hinges on technological relationships, and as such it should therefore have nothing to do with either volcanic or solar activity.

For each draw from the posterior distribution of the model's parameters, I impose the following restrictions on the IRFs of the four shocks I am interested in, $\epsilon_t^{\Delta y}$, ϵ_t^A, ϵ_t^V, and ϵ_t^S:

- a positive $\epsilon_t^{\Delta y}$ produces non-negative IRFs at all horizons for GDP, anthropogenic RF, JRF, global temperatures, the sea level, and ice cover.
- Positive ϵ_t^A, ϵ_t^V, and ϵ_t^S produce non-negative IRFs at all horizons for anthropogenic RF, volcanic RF, and solar RF respectively. Any of the three shocks produces non-negative IRFs at all horizons for JRF, global temperatures, the sea level, and ice cover.

Finally, for each draw from the posterior distribution I impose the restriction that a unitary increase in JRF due to any of the four shocks produces the *same impulse vector* at t=0 for temperatures, sea level, and ice cover. That is, if ΔJRF_0=1 in response to either $\epsilon_t^{\Delta y}$, ϵ_t^A, ϵ_t^V, or ϵ_t^S, then ΔT_0=a, ndΔS_0=b, and ΔI_0=$-c$ for any of the four shocks, with a, b, c>0. The rationale is the same that justifies aggregating the radiative forcing of individual climate change drivers into a single index, the JRF. As previously discussed, evidence suggests that the *specific source* of radiative forcing is irrelevant. In particular, as shown by Kaufmann, Kauppi, and Stock (2006, see Table II and the discussion on page 261), it is not possible to reject the null hypothesis that '*the temperature effect of a unit of radiative forcing (e.g. W/m^2) is equal across forcings*'.

4.1.4 Estimation

I estimate all models via Bayesian methods, based on a straightforward adaptation to the problem at hand of the Metropolis-within-Gibbs algorithm proposed by Justiniano and Primiceri (2008) to estimate DSGE models with stochastic volatility. The algorithm is described in detail in Online Appendix D. In this sub-section I only briefly describe its main features.

Justiniano and Primiceri's (2008) algorithm (see their Appendix A) consisted of two 'blocks' of steps. In Block I the stochastic volatilies of the structural disturbances, and their hyper-parameters, were drawn conditional on the parameters of the DSGE models via a Gibbs step. In Block II a Metropolis step was used in order to draw the DSGE model's parameters conditional on the stochastic volatilities. Within the

present context, in Block II, instead of drawing the parameters of the DSGE models, I draw the parameters of the VAR (9), again via a Metropolis step. As for step I, the only difference with Justiniano and Primiceri (2008) is that I use a simpler specification for the stochastic volatilities. Instead of using their mixture of distributions, I postulate that any of the volatilities of the structural innovations evolves as in Jacquier, Polson, and Rossi (2002).

I run a burn-in pre-sample of 1,000,000 draws which I then discard. I then generate 10,000,000 draws, which I 'thin' by sampling every 1,000 draws in order to reduce their autocorrelation. This leaves 10,000 draws from the ergodic distribution which I use for inference. For all models the fraction of accepted draws is very close to the ideal one, in high dimensions, of 0.23 (see Gelman, Carlin, Stern, and Rubin, 1995). I check convergence of the Markov chain based on Geweke's (1992) inefficiency factors (IFs) of the draws from the ergodic distribution for each individual parameter. For all parameters the IFs are equal to at most 3-4, well below the values of 20-25 which are typically taken to indicate problems in the convergence of the Markov chain.

4.1.5 Restrictions imposed in estimation

In estimation I impose the restrictions that, for each parameters' draw from the posterior distribution, shocks generating permanent increases in either anthropogenic RF (i.e., $\epsilon_t^{\Delta y}$ and ϵ_t^A), or the RF of solar irradiance (ϵ_t^S), generate non-negative IRFs at all horizons for the respective series, i.e. anthropogenic RF and the RF of solar irradiance, respectively. Finally, I restrict the response of volcanic RF to volcanic RF shocks (ϵ_t^V) to be negative at all horizons.

5 Evidence

5.1 Trend GDP growth and the relationship between GDP and anthropogenic emissions

The first panel of Figure 3 shows world real GDP growth and the two-sided median estimate of its time-varying trend μ_t, together with the 16-84 and 5-95 per cent credible sets of the posterior distribution. The estimate of μ_t has been computed via the Monte Carlo integration procedure proposed by Hamilton (1986). Based on the median estimate, trend growth had progressively increased from slightly more than 1 per cent in the 1850s to slightly more than 2 per cent in the aftermath of WWII; it had further accelerated, reaching a peak of about 3.5 per cent in the mid-1960s; and it has decreased ever since, reaching about 2.5 per cent at the end of the sample.

The remaining two panels of Figure 3 show either the one- or the two-sided median estimates of the anthropogenic RF intensity of GDP, i.e. β_t, together with their 16-84 and 5-95 per cent credible sets. Consistent with the evidence in the second and third panels of Figure 1, until WWI the *negative* impact on anthropogenic RF of

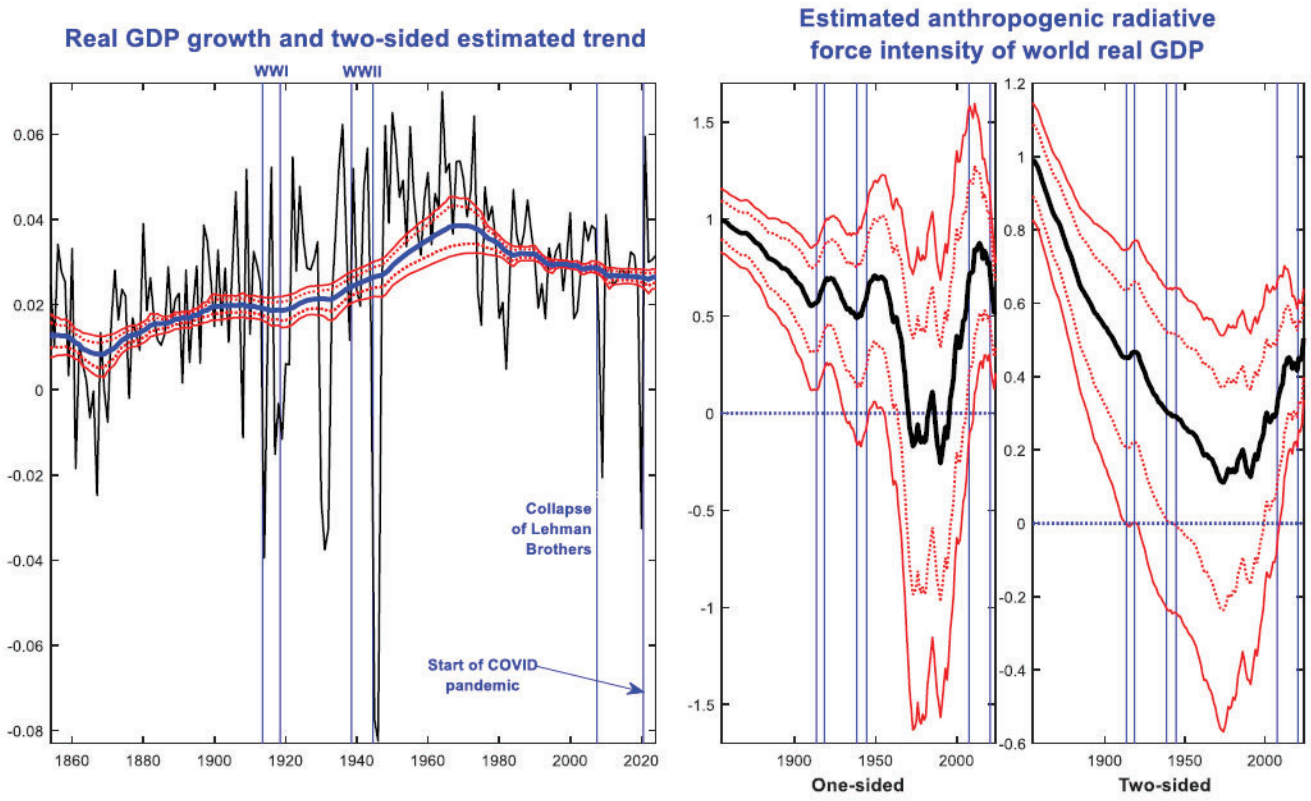

Figure 3 World real GDP growth and two-sided estimate of its trend, and one- and two-sided estimates of the anthropogenic radiative force intensity of GDP (median, and 16-84 and 5-95 credible set)

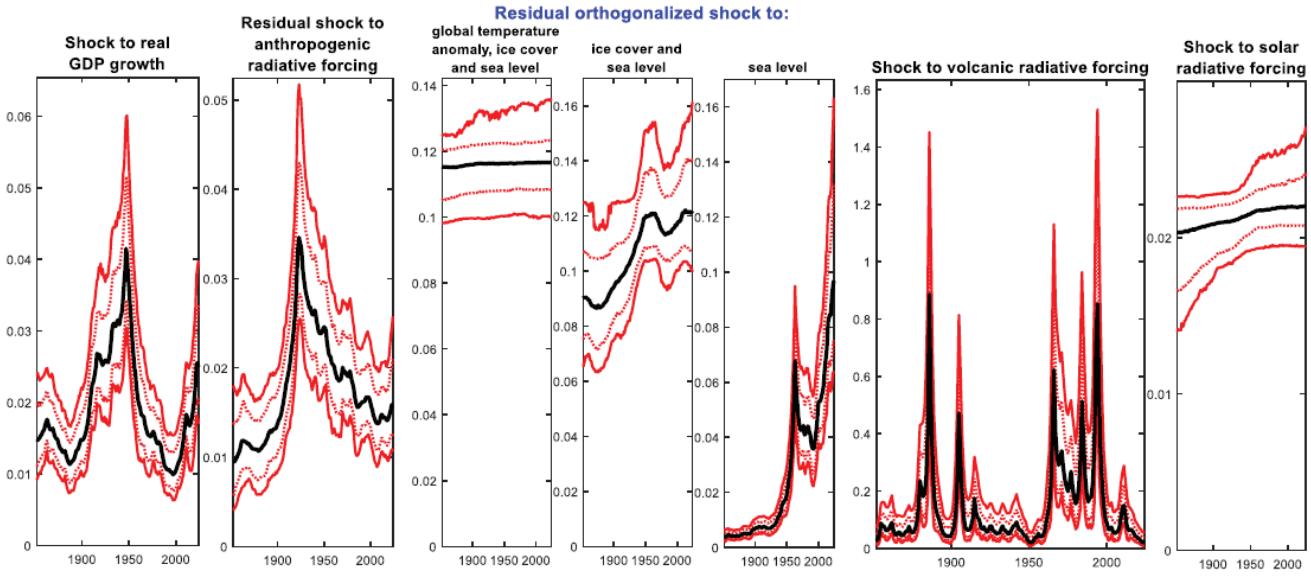

Figure 4 Estimated standard deviations of structural shocks (median, and 16-84 and 5-95 credible sets)

the accumulation of sulphur emissions in the atmosphere roughly balanced out the *positive* impact of the remaining anthropogenic CCDs. As a result, as shown in the third panel of Figure 1, the JRF index *net* of the impact of volcanic emissions had remained essentially constant. Since solar irradiance plays a minor role, this implies that anthropogenic RF had also remained virtually unchanged between the mid-XIX century and WWI. This is why the one-sided estimate in the second panel of Figure 3 exhibits modest variation until WWI. Between the aftermath of WWII and the 1970s, on the other hand, the accumulation of sulphur emissions had dominated other anthropogenic CCDs, with the result that the anthropogenic RF intensity of GDP had dramatically *decreased* to zero. This is consistent with the fact that, in the third panel of Figure 1, the JRF index net of volcanic emissions had decreased during those years. Finally since the 1980s the removal of sulphur from the atmosphere contributed to the increase in anthropogenic RF, with the result that anthropogenic RF intensity has dramatically shot up.

5.2 The volatilities of the structural shocks

Figure 4 shows the estimated standard deviations of the seven identified structural disturbances. For two of them—the shock to solar RF, and the residual orthogonalized shocks to temperatures, ice cover and sea level—the volatility has been virtually unchanged over the entire sample period. At the other extreme, in line with the evidence in the first panel of Figure 1, the volatility of shocks to volcanic RF has exhibited a dramatic extent of variation, which closely mirrors the negative spikes in Figure 1. The standard deviation of innovations to real GDP growth exhibits a roughly hump-shaped pattern, with an increase starting from the early XX century, a peak around World War II, and a sharp fall in the 1950s. Starting from the early XXI century, the shocks of the financial crisis and then of the COVID pandemic have led to a progressive increase. Finally, the standard deviation of the residual shock to anthropogenic RF (i.e. ϵ_t^A) exhibits an even clearer hump-shaped pattern, with a peak reached roughly around World War I.

5.3 Impulse-response functions to radiative forcing shocks

Figure 5 shows the series' IRFs to radiative forcing shocks. For each draw from the posterior distribution I normalize the IRFs to either anthropogenic or solar RF shocks by the long-run impact on anthropogenic and solar RF, respectively. On the other hand, since volcanic RF shocks are transitory, I normalize their IRFs by the impact on volcanic RF at t=0.

Following an exogenous shock to anthropogenic RF, i.e. ϵ_t^A, anthropogenic RF itself essentially reaches its new long-run equilibrium in about two decades, whereas the response of temperatures, the sea level and ice cover is more drawn out and inertial.

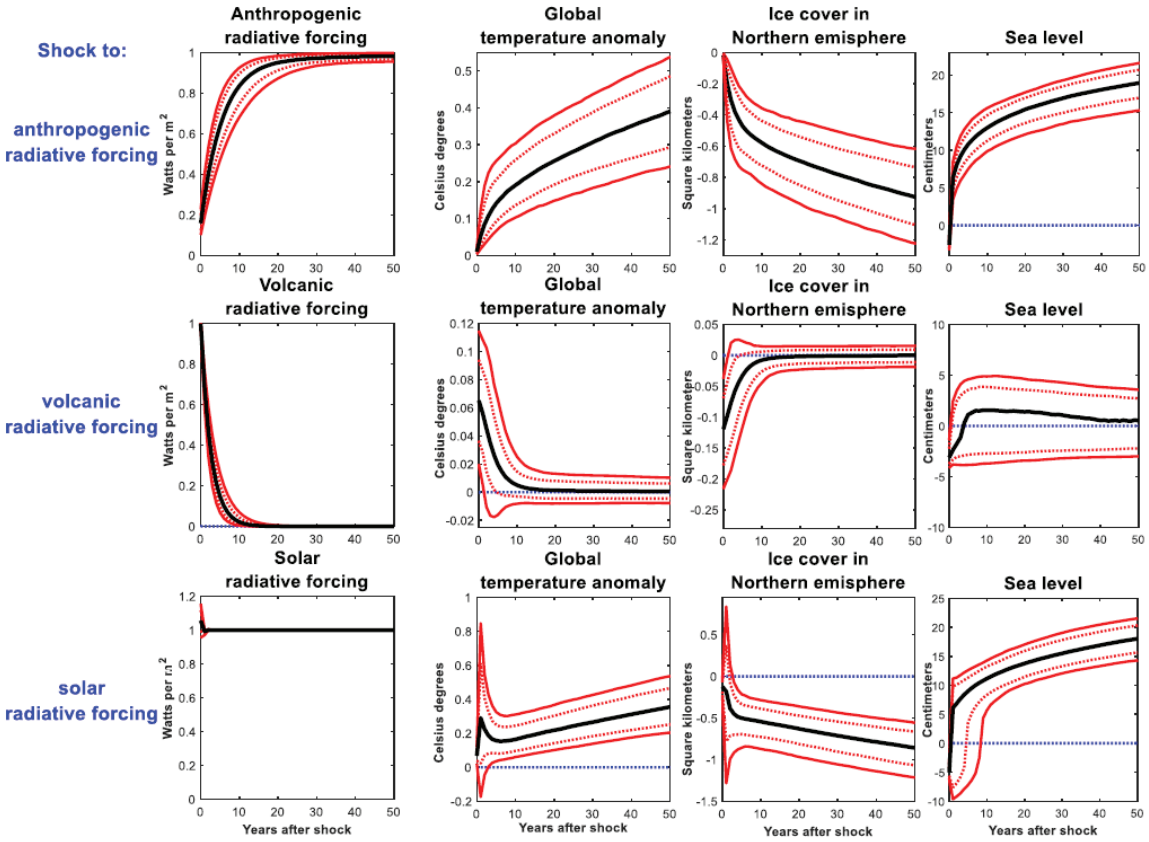

Figure 5 Impulse-response functions to the three identified shocks to radiative forcing (median, and 16-84 and 5-95 credible set)

As one would expect from the first panel of Figure 1, the response of volcanic RF to ϵ_t^V reverts to zero very quickly, in slightly more than ten years. The responses of temperatures, ice cover and sea level are significant on impact, but they quickly become insignificant just a few years later. As for the sea level, it is barely significant even on impact.

Finally, the response of solar RF to ϵ_t^S is virtually flat at all horizons, thus showing that this series is essentially a pure unit root process. The responses of temperatures, ice and sea level are, as expected, drawn out, although with a different profile from the IRFs to ϵ_t^A.

5.4 Unconditional forecasts under 'no change' scenarios

Figure 6 shows evidence from the following exercise. I 'freeze' the state of the system—in particular, both the level of GDP, and the estimate of β_t—at 2024, and I then stochastically simulate the model forward until the end of the XXI century. The evidence from this exercise is sobering. Under such 'no change' scenario, median forecasts predict the temperature anomaly to reach nearly 5 Celsius degrees by 2100, respectively, with the 90%-coverage credible set equal to [3.8; 6.1] degrees. The forecasts for the sea level and ice cover are equally ominous, with the median projection for the former reaching 48 centimeters in 2100, and the 90%-coverage credible set for the latter reaching nearly zero—i.e., *no ice in the Northern emisphere*—at the end of the century.

5.5 Forecasts conditional on alternative assumptions about the evolution of GDP and anthropogenic RF intensity

Figure 7 shows evidence from the following exercise. I 'freeze' once again the state of the system at 2024, and I then stochastically simulate the model forward until the end of the XXI century (1) keeping GDP at its 2024 level, and (2) assuming *full decarbonization* of the world economy in 2025. The evidence from the exercise is sobering. Even if we were somehow able to prevent *any* increase in anthropogenic RF after 2024, still, the intrinsic dynamics of the system in response to past JRF increases would produce dangerous levels of warming going forward, with corresponding impacts on sea level and ice cover. Focusing on global temperatures, about two-thirds of the density of the forecast for 2100 is above the benchmark of the Paris climate agreements of 1.5 Celsius degrees, with a median projection equal to 1.7 degrees, and the upper limit of the 90 per cent-coverage credible set equal to 2.2 degrees. It is important to stress that these increases were already 'locked in' by 2024, which implies that CCDs have *already exceeded* the levels climate scientists regard as dangerous. In turn this implies that only bringing the JRF *back* to levels reached sometime before 2024 would allow to bring climate change under control. The obvious question is by how much should the JRF decrease. Figures 8 and 9 provide some tentative answers

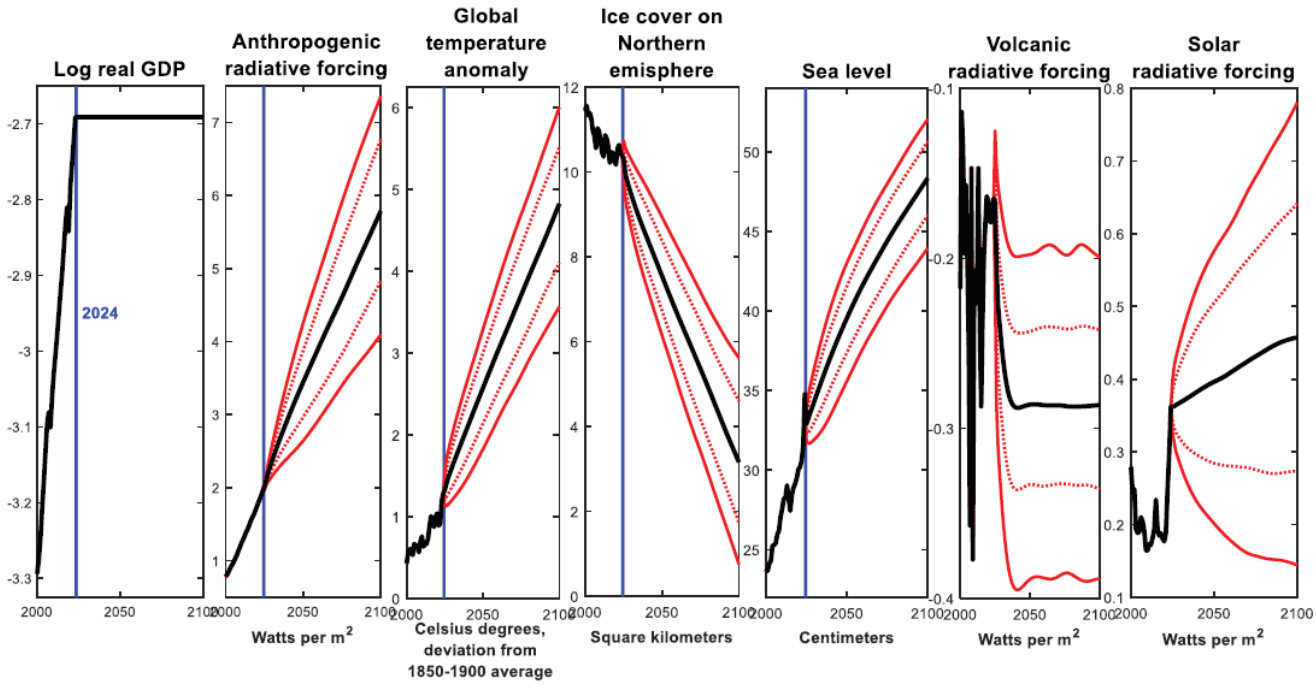

Figure 6 Forecasts keeping both real GDP and its anthropogenic radiative forcing intensity constant at their 2024 levels, (median, and 16-84 and 5-95 credible set)

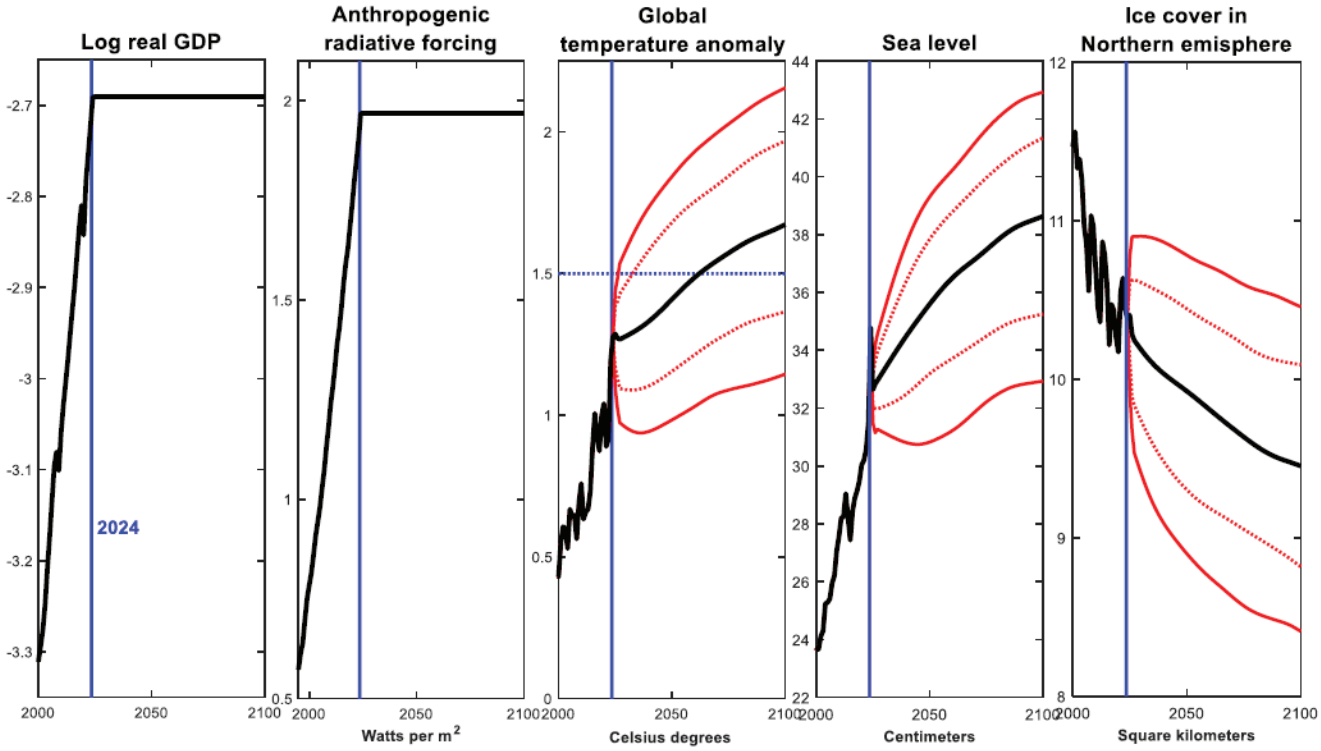

Figure 7 Forecasts keeping real GDP at its 2024 level, and assuming full decarbonization of the economy in 2025 (median, and 16-84 and 5-95 credible set)

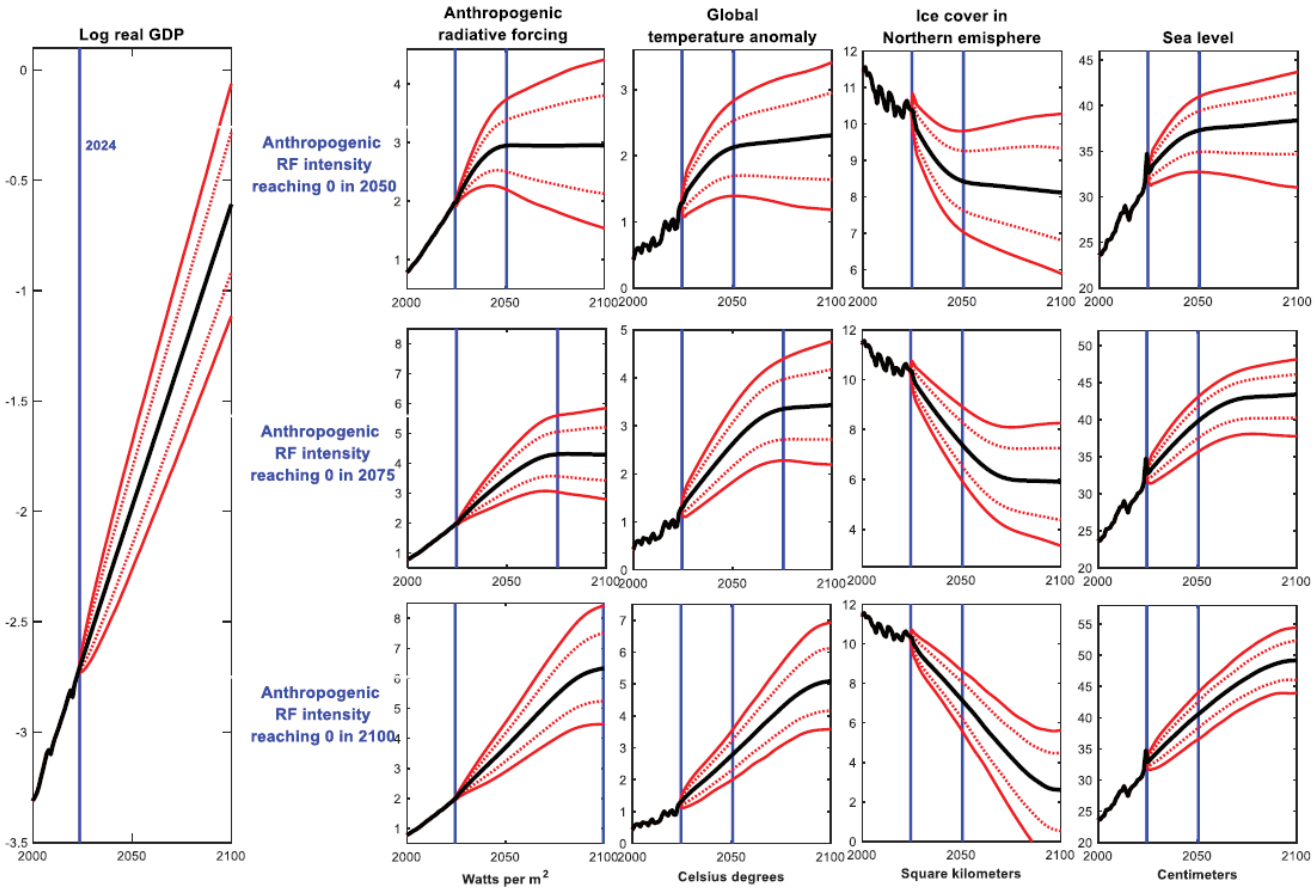

Figure 8 Forecasts with trend real GDP growth after 2024 set to the 2024 estimated value, and decreasing anthropogenic radiative forcing intensity of GDP (median, and 16-84 and 5-95 credible set)

to this question.

Figure 8 shows shows evidence from the following exercise. I 'freeze' trend GDP growth, μ_t, to the estimated value for 2024, and I then simulate the model forward until 2100 conditional on three alternative scenarios for the evolution of anthropogenic RF intensity, in which after 2024 β_t decreases linearly, reaching zero in either 2050, 2075, or 2100. Even the best-case scenario, in which full decarbonization is achieved by 2050, paints a grim picture, with the median forecast for the temperature anomaly reaching a 2.3 Celsius degrees increase compared to pre-industrial times. Further, the upper bound of the 90 per cent-coverage credible set stretches to 3.4 degrees.

5.6 Removing carbon from the atmosphere

Clearly, limiting ourselves to full decarbonization by 2050 is *not enough*, which suggests that, after peaking sometime in the future, anthropogenic RF should be decreased via a massive programme of carbon removal from the atmosphere. The obvious question is: 'To what level should anthropogenic RF be brought back?' Figure 9 provides some evidence on this. The exercise is the same as in Figure 8, with the only difference that after peaking in 2050, anthropogenic RF is then brought back (in terms of its median projection) to the level of the end of the XX century (specifically, 1990). Under this path for anthropogenic RF, the median projection for global temperatures converges to about 0.2. The obvious reason for this 'undershooting' compared to the 1.5 degrees target of the Paris accord is the large extent of uncertainty, with the upper limit of the 90%-coverage credible set being equal to 1.5 degrees.

6 Conclusions

In this paper I use Bayesian VARs with stochastic volatility to forecast global temperatures, sea level, and ice cover in the Northern emisphere until 2100 by exploiting (i) their long-run equilibrium relationship with climate change drivers (CCDs) and (ii) the relationship between world GDP and anthropogenic CCDs. Assuming that trend GDP growth will remain unchanged after 2024, and the world economy will fully decarbonize by 2050, global temperatures and the sea level are projected to increase by 2.5 Celsius degrees and 45 centimeters respectively compared to pre-industrial times. Further, uncertainty is substantial, pointing to significant upward risks. Because of this, bringing climate change under control will require a massive programme of carbon removal from the atmosphere, in order to bring anthropogenic CCDs back to the levels of the end of the XX century.

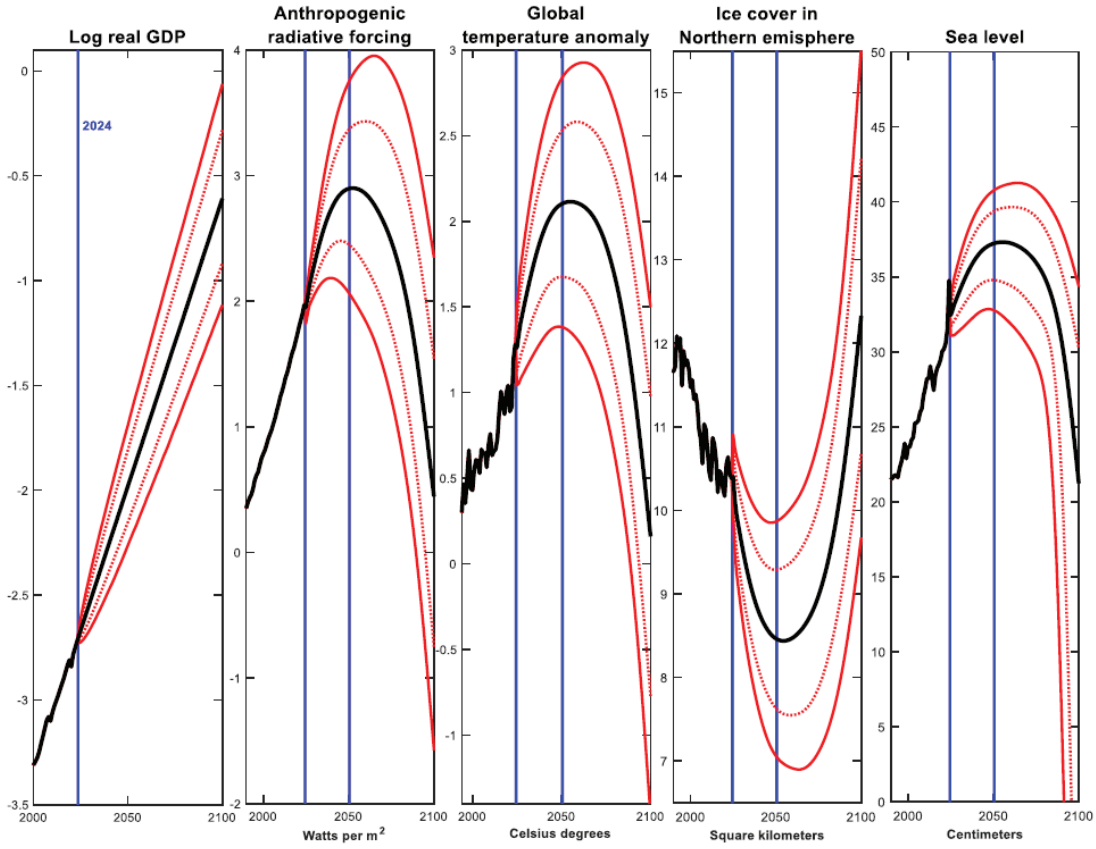

Figure 9 Forecasts with trend real GDP growth after 2024 set to the 2024 estimated value, and the anthropogenic radiative forcing intensity of GDP peaking at 2050 and then decreasing (median, and 16-84 and 5-95 credible set)

7 References

An, S., and Schorfheide, F. (2007): "Bayesian Analysis of DSGE Models", *Econometric Reviews*, 26, 113-172.

Anderson, T.W. (1951), "Estimating Linear Restrictions on Regression Coefficients for Multivariate Normal Distributions", *Annals of Mathematical Statistics*, 22, 327-351.

Bauwens, L., and M. Lubrano (1996): "Identification Restrictions and Posterior Densities in Cointegrated Gaussian VAR Systems", in Advances in Econometrics 11, Part B (JAI Press, Greenwich), 3-28

Beltrao, K. and P. Bloomfield (1987): "Determining the Bandwidth of a Kernel Spectrum Estimate", *Journal of Time Series Analysis*, 8(1), 21-38.

Benati, L. (2007): "Drift and Breaks in Labor Productivity", *Journal of Economic Dynamics and Control*, 31, 2847-2877.

Benati, L. (2008): "Investigating Inflation Persistence Across Monetary Regimes", *Quarterly Journal of Economics*, 123(3), 1005-1060.

Bruns, S.B., Csereklyei, Z. and Stern, D.I. (2020): "A Multicointegration Model of Global Climate Change", *Journal of Econometrics*, 214, 175-197.

Butler, J.H., and Montzka, S.A. (2018): "The NOAA Annual Greenhouse Gas Index (AGGI)", NOAA Earth System Research Laboratory, Boulder, CO

Cavaliere, G., A. Rahbek, and A. M. R. Taylor (2012): "Bootstrap Determination of the Cointegration Rank in Vector Autoregressive Models", *Econometrica*, 80(4), 1721-1740.

Church, J.A., and White, N.J. (2006): "A 20th century acceleration in global sea-level rise", *Geophysical Research Letters*, 33, L01602.

Cochrane, J.H. (1988): "How Big Is the Random Walk in GNP?", *Journal of Political Economy*, 96(5), 893-920

Coddington, O., Lean, J.L., Pilewskie, P., Snow, M., Lindholm, D. (2015): "A Solar Irradiance Climate Data Record", *Bulletin of the American Meteorological Society*, p. 1265-1282.

Corana, A., Marchesi, M., Martini,C., and Ridella, S. (1987): "Minimizing Multimodal Functions of Continuous Variables with the Simulated Annealing Algorithm," *ACM Transactions on Mathematical Software*, 13.

Dergiades, T., Kaufmann, R.K., Panagiotidis, T. (2016): "Long-Run Changes in Radiative Forcing and Surface Temperature: The Effect of Human Activity Over the Last Five Centuries", *Journal of Environmental Economics and Management*, 76, 67-85.

Diebold, F.X. and Chen, C. (1996): "Testing Structural Stability with Endogenous Breakpoint: A Size Comparison of Analytic and Bootstrap Procedures", *Journal of Econometrics*, 70(1), 221-241.

Elliot, G., T.J. Rothenberg and J.H. Stock (1996): "Efficient Tests for an Autoregressive Unit Root", *Econometrica*, 64(4), 813-836.

Engle, R. F., and C. W. Granger (1987): "Cointegration and Error Correction: Representation, Estimation, and Testing", *Econometrica*, 55(2), 251-276.

Franke, J. and W. Hardle (1992): "On Bootstrapping Kernel Spectral Estimates", *Annals of Statistics*, 20(1), 121-145.

Gadea, M.D. and J. Gonzalo (2024), "Long-Term Climate forecasts", Universidad de Zaragoza and Universidad Carlos III, mimeo

Gelman, A., Carlin, J.B., Stern, H.S., and Rubin, D. (1995): *Bayesian Data Analysis*, New York, Chapman and Hall.

Geweke, J. (1992): "Evaluating the accuracy of sampling-based approaches to the calculation of posterior moments", in J. M. Bernardo, J. Berger, A. P. Dawid and A. F. M. Smith (eds.), *Bayesian Statistics*, Oxford University Press, Oxford, pages 169-193.

Giannone, D., Lenza, M., and Primiceri, G. (2019): "Priors for the Long Run", *Journal of the American Statistical Association*, 114:526, pp. 565-580.

Goffe, W.L., Ferrier, G., and Rogers, J. (1994): "Global Optimization of Statistical Functions with Simulated Annealing", *Journal of Econometrics*, 60, 65-99.

Hamilton, J.D. (1986): "A Standard Error for the Estimated State Vector of a State-Space Model", *Journal of Econometrics*, 33(3), 387-397.

Kaufmann, R.K. and D.I. Stern (2002), "Cointegration Analysis of Hemispheric Temperature Relations", *Journal of Geophysical Research*, Vol. 107, N. D2, 4012, 10.1029/2000JD000174.

Kaufmann, R.K., H. Kauppi, and J.H. Stock (2006): "Emissions, Concentrations, and Temperature: A Time Series Analysis", *Climatic Change*, 77: 249-278.

Kaufmann, R.K., H. Kauppi, and J.H. Stock (2010): "Does Temperature Contain a Stochastic Trend? Evaluating Conflicting Statistical Results", *Climatic Change*, 101:395-405.

Kaufmann, R.K., H. Kauppi, M.L. Manna, and J.H. Stock (2011), "Reconciling Anthropogenic Climate Change with Observed Temperature 1998–2008, PNAS, July 19, 2011, Vol. 108, n. 29.

Kleibergen, F. and H.K. van Dijk (1994): "On the Shape of the Likelihood/Posterior in Cointegration Models", *Econometric Theory*, 10, 514-551.

Koop, G., Strachan, R., van Dijk, H., and Villani,M. (2006): "Bayesian Approaches to Cointegration", in K. Patterson and T. Mills, editors, *The Palgrave Handbook of Theoretical Econometrics*, Palgrave MacMillan

Koop, G., Léon-González, R., and Strachan, R.W. (2010): "Efficient Posterior Simulation for Cointegrated Models with Priors on the Cointegration Space", *Econometric Reviews*, 29(2), 224-242

Kopp, G. and G. Lawrence (2005): "The Total Irradiance Monitor (TIM): Instrument Design", *Solar Physics*, 230(1), 91-109.

Kopp, G, K. Heuerman, and G. Lawrence (2005): "The Total Irradiance Monitor (TIM): Instrument Calibration", *Solar Physics*, 230(1), 111-127.

Kopp, G., Krivova, N., Lean, J., and C.J. Wu (2016): "The Impact of the Revised Sunspot Record on Solar Irradiance Reconstructions", *Solar Physics*, p. 1-18.

Jacquier, E., Polson, N.G., and Rossi, P.E. (2007): "Bayesian Analysis of Stochastic Volatility Models", *Journal of Business & Economic Statistics*, Vol. 20, No. 1, Twentieth Anniversary Commemorative Issue (Jan., 2002), pp. 69-87.

Johansen, S. (1988), "Statistical Analysis of Cointegration Vectors", *Journal of Economic Dynamics and Control*, 12, 231-254.

Johansen, S. (1991), "Estimation and Hypothesis Testing of Cointegration Vectors in Gaussian Vector Autoregressive Models", *Econometrica*, 69, 111-132.

Johansen, S. (1992), "A Representation of Vector Autoregressive Processes Integrated of Order 2", *Econometric Theory*, 8(2), 188-202.

Johansen, S. (1995), "A Statistical Analysis of Cointegration for I(2) Variables", *Econometric Theory*, 11(1), 25-59.

Johansen, S. (1997), "Likelihood Analysis of the I(2) Model", *Scandinavian Journal of Economics*, 24(4), 433-462.

Joshi, M.M., Gregory, J.M., Webb, M.J., Sexton, D.M.H., and Johns, T.J. (2008): "Mechanisms for the land/sea warming contrast exhibited by simulations of climate change", *Climate Dynamics*, Vol. 30, 455-465.

Juselius, K. (2006), *The Cointegrated VAR Model: Methodology and Applications*, Oxford University Press.

Justiniano, A. and Primiceri, G.E. (2008): "The Time-Varying Volatility of Macroeconomic Fluctuations", *American Economic Review*, 98:3, 604-641.

Lambert, F.H., Webb, M.J., and Joshi, M.M. (2011): "The Relationship between Land–Ocean Surface Temperature Contrast and Radiative Forcing", *Journal of Climate*, Vol. 24 (July), 3239-3256.

Liu, H., and Rodriguez, G. (2005): "Human Activities and Global Warming: A Cointegration Analysis", *Environmental Modelling & Software*, 20, 761-773.

Luetkepohl, H. (1991): *Introduction to Multiple Time Series Analysis*, 2nd edition. Springer-Verlag.

Mann, M. (2023): *Our Fragile Moment: How Lessons from the Earth's Past Can Help Us Survive the Climate Crisis*, Scribe, Melbourne and London.

Nyblom, J. (1989), "Testing for the Constancy of Parameters Over Time", *Journal of the American Statistical Association*, 84(405), 223-230.

Robertson, A., Overpeck, J., Rind, D., Mosley-Thompson, E., Zielinski, G., Lean, J., Koch, D., Penner, J., Tegen, I., and Healy, R. (2001): "Hypothesized Climate Forcing Time Series for the Last 500 Years", *Journal of Geophysical Resesearch Atmosphere*, Vol. 106(D14), p. 14, 783.

Schallock, J., Brühl, C., Bingen, C., Höpfner, M., Rieger, L., and Lelieveld, J. (2023): "Reconstructing volcanic radiative forcing since 1990, using a comprehensive emission inventory and spatially resolved sulfur injections from satellite data in a chemistry-climate model", *Atmospheric Chemistry and Physics*, 23, 1169-1207.

Shine, K.P.R.G., Derwent, D.J., Wuebbles, D.J., and Mocrette, J.J. (1991): "Ra-

diative Forcing of Climate", in Houghton, J.T., Jenkins, G.J., and Ephramus, J.J., editors, *Climate Change: The IPCC Scientific Assessment*, Cambridge University Press, Cambridge, pp. 47-68.

Stern, D.I. and Kaufmann, R.K. (2000): "Detecting a Global Warming Signal in Hemispheric Temperature Series: A Structural Time Series Analysis", *Climatic Change*, 47, 411-438.

Stern, D.I. and Kaufmann, R.K. (2014): "Anthropogenic and Natural Causes of Climate Change", *Climate Change*, 122, 257-269.

Stock, J. and Watson, M. (1996): "Evidence of Structural Instability in Macroeconomic Time Series Relations", *Journal of Business and Economic Statistics*, 14(1), 11-30.

Stock, J. and Watson, M. (1998): "Median-Unbiased Estimation of Coefficient Variance in a Time-Varying Parameter Model", *Journal of the Americal Statistical Association*, 93(441), 349-358.

Strachan, R. and Inder, B. (2004): "Bayesian Analysis of the Error Correction Model", *Journal of Econometrics*, 123, 307-325.

Sutton, R.T., Dong, B., and Gregory, J.M. (2007): "Land/sea warming ratio in response to climate change: IPCC AR4 model results and comparison with observations", *Geophysical Research Letters*, Vol. 34, L02701.

Waggoner, D.F. and Zha, T. (1999): "Conditional Forecasts in Dynamic Multivariate Models", *Review of Economics and Statistics*, 81(4), 639-651.

Figures for Appendix

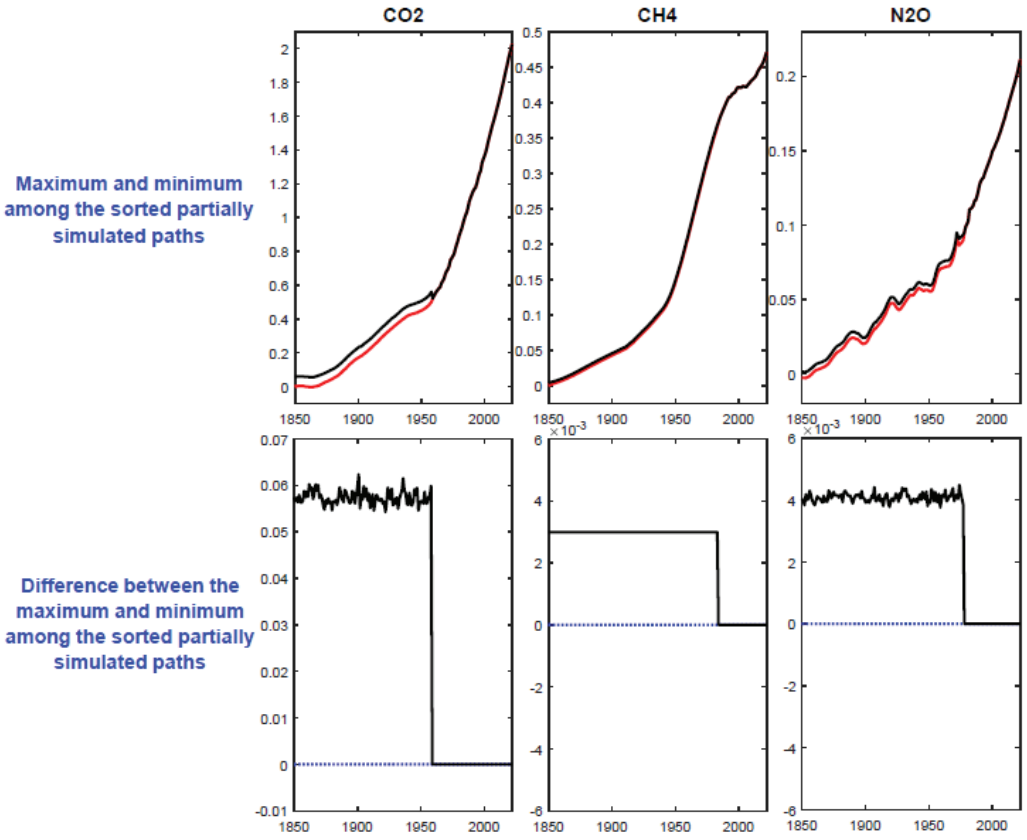

Figure A.1 Evidence on the close similarity between alternative partially simulated series for CO2, NH4, and N2O: maximum and minimum among the sorted partially simulated paths out of 100,000 simulations

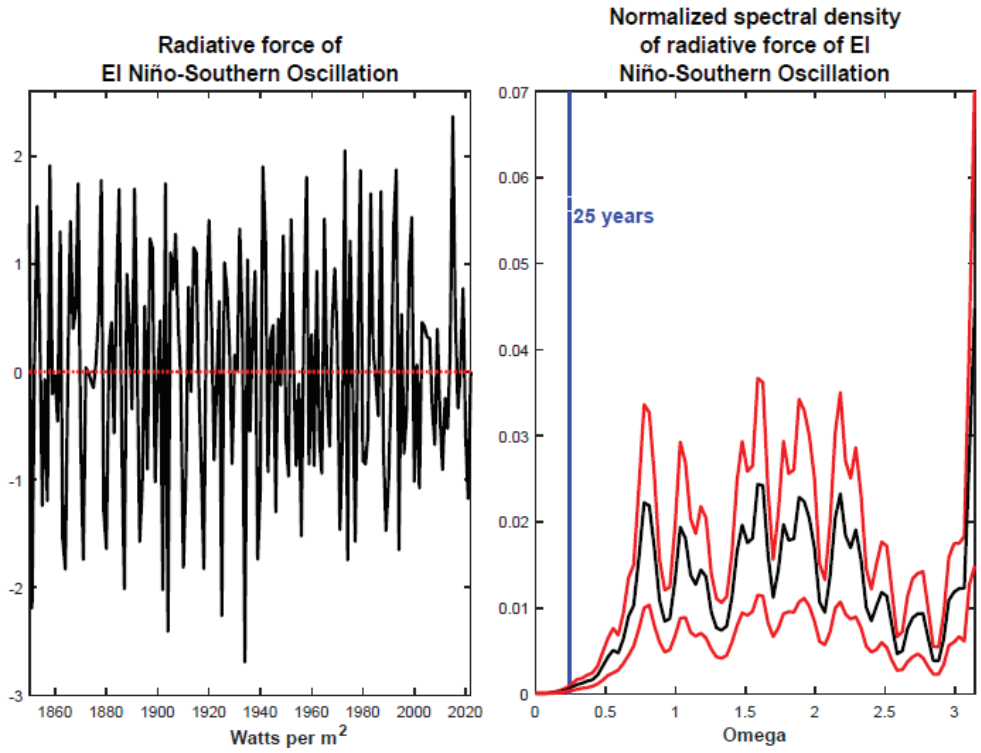

Figure A.2 Radiative force of El Niño-Southern Oscillation: raw series and normalized spectral density (with 90%-coverage bootstrapped confidence bands)

Online Appendix for: World GDP, Anthropogenic Emissions, and Global Temperatures, Sea Level, and Ice Cover

Luca Benati
University of Bern*

A The Data

A.1 Data sources

A.1.1 Temperature anomalies

Annual data since 1850 (January-December averages, in Celsius degrees) for the global land and ocean temperature anomalies, as well as for the global overall anomaly (i.e., both land and ocean) are from the website of the U.S. National Oceanic and Atmospheric Administration (NOAA) at: https://www.ncei.noaa.gov/. They are expressed as deviations from the 1901-2000 average. Since the standard reference period used first and foremost by the Intergovernmental Panel on Climate Change (IPCC) is 1850-1900, I adjust the NOAA series by rescaling them accordingly.

A.1.2 Climate change drivers

I consider nine drivers of climate change: CO2, methane (CH4), nitrous oxide (N2O), chlorofluorocarbons (CFC11 and CFC12), anthropogenic sulfur emissions (SOx), El Niño and La Niña (El Niño-Southern Oscillation, henceforth ENSO), solar irradiance, and volcanic activity. In line with both the climate science literature, and the literature on the econometrics of climate change, I convert (as detailed below) each CCD into 'Radiative Forcing' (RF), which provides a precise numerical measure, expressed in Watts per square meter (Watts/m^2), of the ability of individual CCDs to trap heat in the atmosphere. As it is standard in the literature, I do this based on formulas from physics (see below).

Starting from *anthropogenic* climate change drivers (CCDs), data sources are as follows. As for CO2, data before 1958 have been spline-interpolated based on the data retrieved from the Scripps CO2 Program (at http://scrippsco2.ucsd.edu). Since 1958, data are based on direct measurements from the Mauna Loa observatory. As for CH4, until 1997 data are from Robertson at el. (2001). Since then they are from NOAA. As for N2O, until 2017 data are from https://www.n2olevels.org/. Since then they are from NOAA. The concentrations of

*Department of Economics, University of Bern, Schanzeneckstrasse 1, CH-3001, Bern, Switzerland. Email: luca.benati@vwi.unibe.ch

CO2, CH4, and N2O in the atmosphere have been converted into radiative forcing based on the formulas found in Table 1 of Butler and Montzka (2018).

Data on the radiative forcing of chlorofluorocarbons (CFC11 and CFC12) are from Stern and Kaufmann (2014), and they have been updated based on data from NOAA and the formulas for radiative forcing found in Stern and Kaufmann (2000, p. 435).

A series for the radiative forcing of anthropogenic sulfur emissions (SOx) is from Stern and Kaufmann (2014), and it has been updated based on data from the OECD and the formulas for radiative forcing found in Stern and Kaufmann (2000, p. 435).

Turning to *non anthropogenic* drivers of climate change, data on solar irradiance are from Coddington et al. (2015) and Kopp et al. (2016) until 2014. Since then they are from the SORCE Total Irradiance Monitor (TIM).[1] I convert the resulting index of solar irradiance into radiative forcing based on the formula found on p. 435 of Stern and Kaufmann (2000), which in turn is based on the IPCC (see Shine et al. 1991). Since solar irradiance features an 11-years cycle which is irrelevant for the present purposes, I remove it via the band-pass filter proposed by Christiano and Fitzgerald (2003).[2] An index of volcanic forcing (i.e., radiative forcing originating from volcanic eruptions) is from Dergiades et al. (2016) until 1979. After that it is from Schmidt et al. (2016) and from the updated dataset of Schallock et al. (2023). Finally, the radiative forcing of El Niño and La Niña (El Niño-Southern Oscillation, henceforth ENSO) is from Dergiades, Kaufmann, and Panagiotidis (2016) until 2011, and it has been updated based on data from NOAA.

A.1.3 World real GDP

Annual data for world real GDP since 1850 are from sfu.ca/~djacks/data/publications/index.html until 1980. Since then, they have been reconstructed based on the annual growth rates from the International Monetary Fund's World Economic Outlook database.

A.1.4 World sea level

An annual series for the world sea level since 1801 has been constructed as follows. Since 1880, data are from the U.S. Environmental Protection Agency's (EPA) Climate Change Indicators (see at: www.epa.gov/climate-indicators). Between 1870 and 1880 data are from Church and White (2006). Finally, for the period 1801-1869 I proceed as follows. Annual sea level data for Amsterdam, Brest, and Stockholm are available since 1766, 1711, and 1801 respectively, but for each series a few years are missing. For the period 1874-1923, for which both the world sea level series and any of the series for three cities are all available, I run an OLS regression of the world sea level series on a constant and the sea level series for Amsterdam, Brest, and Stockholm. Finally, I compute a world sea level proxy for the period 1801-1871 as the predicted value which is obtained by applying the coefficients from OLS regression to the actual values for the three cities' sea level for that period. The overall annual sea level series has been obtained by linking the three previously described series. Specifically, it is equal to the just-mentioned proxy for the period 1801-1869, to the series

[1] Details of the TIM design and calibrations are given in Kopp and Lawrence (2005) and Kopp et al. (2005).

[2] Specifically, since I am working at the annual frequency, I remove the frequency band associated with fluctuations between 10 and 12 years.

from Church and White (2006) for the period 1870-1879, and to the EPA series since 1880. The series is expressed in centimeters.

A.1.5 Ice cover in the Northern emisphere

An annual series for ice cover in the Northern emisphere (in square kilometers) if from NOAA (at https://www.ncei.noaa.gov/access/monitoring/snow-and-ice-extent/sea-ice/N/0) since 1979. Before that it is from Walsh, Chapman, Fetterer, and Stewart (2019).

A.2 Linking data based on regular measurements with interpolated data based on irregular observations

For three climate change drivers—CO2, NH4, and N2O—I link spline-interpolated series based on *irregular* observations with series based on *regular* direct measurements. One obvious concern with doing this is that the two types of data that are being linked are not exactly comparable, and performing econometrics based on the resulting linked series may therefore produce unreliable results. As it is routinely done in the climate science literature, for either CO2, NH4, or N2O I therefore address this issue as follows.

To fix ideas, let us focus on CO2 (the logic for NH4 and N2O is the same). The spline-interpolated series based on data from the Scripps CO2 program is available until 2018, whereas the series based on direct measurements from the Mauna Loa observatory is available since 1958. Over the common sample period, 1958-2018, I estimate an AR(1) process for the difference between the two series. Then, based on standard resampling methods, I bootstrap (i.e., stochastically simulate) the estimated AR(1) process for a sample equal to the length of the sample for the spline-interpolated data (i.e. 1850-2018) and I add it to the spline-interpolated series. In this way I obtain for the 1850-2018 period a series that mimics the stochastic properties of the series based on direct measurement from Mauna Loa for the period since 1958. (This is what in the climate science literature is labelled as 'adding red noise' to an interpolated series.) Finally, I construct the linked series for the overall period 1850-2023 by linking the thus constructed, partially simulated series (until 1957) and the Mauna Loa series (since 1958). For NH4 and N2O I proceed in the same way.

By construction, over the first part of the sample period the linked series for CO2, NH4, and N2O are random, as they depend on the specific realizations of the bootstrapped red noise processes. (In Section A.5 below I discuss how I address this issue via Monte Carlo integration, by integrating out the randomness originating from the bootstrapped red noise processes.) It is to be stressed, however, that because of the comparatively small magnitude of the estimated red noise compared to the *levels* of the series, the difference between individual stochastic simulations is very small.[3] This means that, in practice, what is shown in Figure 1 in the main text of the paper is representative of the entire universe of simulations. Figure A.1 provides simple evidence on this. The figure shows, for CO2, NH4, and N2O, the maximum and the minimum among the sorted partially simulated paths out of 100,000 simulations, together with the difference between them. Evidence is very clear: over the first portions of the sample the simulated paths had been very close. This had especially been the case for CH4, and just slighty less so for CO2 and N2O.

[3]Then, for either CO2, NH4, or N2O the second part of the respective samples, being based on direct regular measurements, is by definition the same.

A.3 Construction of the aggregate Joint Radiative Forcing index

Once each driver of climate change has been converted into radiative forcing, I construct the *aggregate* Joint Radiative Forcing (JRF) index as in Kaufmann, Kauppi, and Stock (2006) by summing up the individual components. As shown by Kaufmann, Kauppi, and Stock (2006, see Table II and the discussion on page 261), it is indeed not possible to reject the null hypothesis that 'the temperature effect of a unit of radiative forcing (e.g. W/m^2) is equal across forcings'. The single exception is ENSO, which I ignore for the reasons I discuss in the next sub-section.

A.4 Why excluding El Niño and La Niña

Figure A.2 shows the radiative forcing of El Niño and La Niña (ENSO), together with its estimated normalized spectral density with 90%-coverage bootstrapped confidence bands.[4] Two main findings are apparent from the figure:

(1) the radiative forcing of ENSO is extraordinarily noisy compared to the radiative forcing of the other drivers of climate change. For example in Figure 1 in the main text of the paper the radiative forcing of the dominant driver of climate change, CO2, goes from zero (by normalization) in 1850 to slightly beyond 2 in 2023. By contrast, the ENSO radiative forcing in Figure A.2 has a standard deviation of 1.0742, and since 1850 it has oscillated from a minimum of -2.69 to a maximum of 2.37.

(2) As the second panel of Figure A.2 clearly illustrates, ENSO's radiative forcing has essentially no spectral power at frequencies beyond 25 years.

The implication of (1) and (2) is that, for the present purposes, including in the JRF index the radiative forcing of ENSO shown in the first panel of Figure A.2 would uniquely add a large amount of comparatively high-frequency noise, whereas it would bring essentially *no information* about the long-horizon, low-frequency developements that are the focus of the present work. To put it differently, this would uniquely complicate the analysis, whereas it would not bring any benefit whatsoever. Because of this, in the construction of the JRF index I have decided to ignore the El Niño and La Niña phenomenon.

A.5 Integrating out simulated red noise via Monte Carlo integration

As discussed, over the first part of the sample period the linked series for CO2, NH4, and N2O are random, as they depend on the specific realizations of the bootstrapped red noise processes. I therefore address this issue as follows.

For $k = 1, 2, 3, ..., K$, with $K = 1{,}000$, I generate partially simulated[5] series for the concentration of CO2, NH4, and N2O in the atmosphere, I convert them into radiative forcing, and I sum them to the radiative forcings of the remaining drivers of climate change, thus obtaining a partially simulated series for the JRF index. Based on this and on the series for the temperature anomalies (which are based on regular direct observations over the entire

[4] I estimate the spectral density by smoothing in the frequency domain the Fast-Fourier-Transform (FFT)-based estimator of the series' periodogram via a Bartlett spectral window. The bandwidth is selected automatically via the procedure proposed by Beltrao and Bloomfield (1987). Spectral bootstrapping is implemented via the procedure proposed by Franke and Hardle (1992). I implement 10,000 bootstrap replications.

[5] Based on the previous discussion, 'partially simulated' refers to the first part of the sample, for which we only have spline-interpolated data.

sample period) I then estimate the VARs, and I compute the median, and the 16-84 and 5-95 percentiles for all of the objects if interest (impulse-response functions to a permanent shock to the level of JRF; unconditional and conditional forecasts; etc.). Finally, I *integrate out* the uncertainty deriving from the fact that for CO2, NH4, and N2O the first part of the sample has been partially simulated by computing the average (corresponding to the expected value) of the objects of interest across all of the K simulations. This Monte Carlo integration procedure allows to perform the empirical analysis by effectively controlling for the fact that three of the radiative forcing series have been partially stochastically simulated.

B Statistical Properties of the Data

B.1 Unit root tests

Tables B.1*a*-B.1*b* show bootstrapped p-values for Elliot, Rothenberg, and Stock's (1996) unit root tests for both the levels and the first differences of climate change series. For all series except the JRF index we have data based on continuous direct measurements for the entire sample since 1850. For these series I therefore perform the tests in the standard way, bootstrapping them as in Diebold and Chen (1996) based on the first difference of the series that is being tested, i.e., either the (log) level or the (log) difference of the original series. I consider five possible lag orders, from 1 to 5 years.

Table B.1*a* Bootstrapped p-values for Elliot, Rothenberg, and Stock's (1996) unit root tests for the anthropogenic radiative forcing index[a]

	p=1	p=2	p=3	p=4	p=5
	Mean of Monte Carlo distribution of p-values				
In levels, without a time trend	1.0000	1.0000	1.0000	1.0000	1.0000
In levels, with a time trend	0.9995	0.9994	0.9992	0.9997	0.9999
In first differences, without time trend	0.0001	0.0032	0.0379	0.1313	0.3018
	Median of Monte Carlo distribution of p-values				
In levels, without a time trend	1.0000	1.0000	1.0000	1.0000	1.0000
In levels, with a time trend	0.9995	0.9995	0.9995	1.0000	1.0000
In first differences, without time trend	0.0000	0.0030	0.0375	0.1305	0.3010
	Fraction of Monte Carlo distribution of p-values smaller than 10 per cent				
In levels, without a time trend	0.0000	0.0000	0.0000	0.0000	0.0000
In levels, with a time trend	0.0000	0.0000	0.0000	0.0000	0.0000
In first differences, without time trend	1.0000	1.0000	1.0000	0.0425	0.0000

[a] Based on10,000 Monte Carlo simulations of joint radiative forcing.

For the JRF index, on the other hand, I generate 10,000 partially simulated series as described in Appendix A.5, and based on each of them I perform the same unit root tests I perform for the other series. Table B.1*a* reports the means and the medians of the Monte Carlo distributions of the bootstrapped p-values across the 10,000 simulations, together with the fraction of Monte Carlo replications for which the p-values are smaller than 10%.

Table B.1*b* Bootstrapped *p*-values for Elliot, Rothenberg, and Stock's (1996) unit root tests for the land and ocean temperature anomalies

	p=1	p=2	p=3	p=4	p=5
	Land temperature anomaly				
In levels, without time trend	0.6824	0.9052	0.9750	0.9904	0.9940
In levels, with time trend	0.1526	0.3048	0.7162	0.7180	0.7308
In first differences, without time trend	0.0000	0.0000	0.0000	0.0000	0.0000
	Ocean temperature anomaly				
In levels, without time trend	0.4682	0.7256	0.9120	0.9296	0.9588
In levels, with time trend	0.1278	0.4878	0.5440	0.5558	0.6766
In first differences, without time trend	0.0000	0.0000	0.0000	0.0000	0.0000
	Overall temperature anomaly				
In levels, without time trend	0.8651	0.9704	0.9926	0.9930	0.9971
In levels, with time trend	0.3687	0.6454	0.7757	0.6099	0.7826
In first differences, without time trend	0.0000	0.0000	0.0000	0.0000	0.0001
	Log real GDP				
In levels, without time trend	0.9891	0.9878	0.9877	0.9707	0.9594
In levels, with time trend	0.0534	0.3759	0.3079	0.3488	0.3919
In first differences, without time trend	0.0000	0.0009	0.0009	0.0009	0.0009
	Volcanic radiative forcing				
In levels, without time trend	0.0000	0.0000	0.0000	0.0004	0.0035
controlling for break in the mean	0.0000	0.0000	0.0000	0.0000	0.0005
	Solar radiative forcing				
In levels, without time trend	0.2665	0.3437	0.4992	0.5889	0.6648
In levels, with time trend	0.0147	0.0195	0.0516	0.0837	0.2282
In first differences, without time trend	0.0000	0.0000	0.0000	0.0001	0.0000
	Ice cover				
In levels, without time trend	0.0000	0.0028	0.0258	0.1489	0.3495
In levels, with time trend	0.0000	0.0000	0.0003	0.0214	0.0656
In first differences, without time trend	0.0000	0.0000	0.0000	0.0000	0.0002
	Sea level				
In levels, without time trend	0.9872	0.9925	0.9955	0.9962	0.9999
In levels, with time trend	0.9559	0.8853	0.9317	0.9129	0.9367
In first differences, without time trend	0.0009	0.0173	0.1146	0.2712	0.4303

For all series except volcanic RF the null of a unit root cannot be rejected in levels, either including or not including a time trend, and based on any of the five lag orders. The only exception is ice cover, for which a unit root is rejected when including a time trend. Since the most plausible alternative is a model not including a time trend,[6] in what follows I downplay these results, and I assume that ice cover, too, feature a unit root. For volcanic RF rejection of the null is very strong, either not controlling or controlling for the break in the mean in 1961 identified by Bai-Perron tests.

In differences a unit root is strongly rejected for all series except the JRF index and the sea level. For the JRF index it is rejected at the 10 per cent level only for lag orders smaller than or equal to 3, whereas for the sea level it is rejected only for lag orders smaller than or equal to 2.

Based on the evidence in Tables B.1*a*-B.1*b* a reasonable characterization of the data, which has in fact been adopted by the vast majority of cointegration-based studies on climate change (see the discussion Sections 1.1 and 1.2.2 in the main text of the paper), is that all of the series are I(1). As the evidence in the next sub-section shows, however, this conclusion would most likely be incorrect, since Stock and Watson's (1996, 1998) tests applied to the first differences of the series strongly suggest that they all contain a random-walk component.

B.2 Searching for random-walk time-variation in the first differences of the series

Table B.2 report evidence from Stock and Watson's (1996, 1998) tests of the null hypothesis of no time-variation in the mean of the first difference of any of the series, against the alternative of random-walk time variation. For volcanic radiative forcing I control for the break in the mean in 1961 identified by Bai-Perron tests. In implementing Stock and Watson's approach I closely follow Stock and Watson (1996, 1998). The methodology is described in detail in Appendix C, and it is exactly the same I used in Benati (2007). I consider three alternative values of 'trimming', i.e. the standard 15% and, in order to give more power to the tests, either 25% or 33%. I control for the possible autocorrelation and/or heteroskedasticity of the residuals via either Newey and West's (1987) or Andrews' (1991) covariance matrix estimator. For all series except the JRF index I simply report the simulated p-values produced by Stock and Watson's methodology. For the JRF index I report the mean and the median of the Monte Carlo distribution of the simulated p-values, together with the fraction of the p-values smaller than 10%, across 10,000 Monte Carlo simulations.

For both volcanic and solar radiative forcing the null of time invariance in the mean of the first difference of the series cannot be rejected, with p-values ranging between 0.22 and 0.915. For the ice cover index evidence is mixed, with three p-values out of six smaller than 10 per cent. For all other series I consistently detect strong evidence of random-walk time-variation. This suggests that although for these series the I(1) component is too small to be detected based on standard unit root tests, in fact it is sufficiently large to be detected based on the approach proposed by Stock and Watson (1996, 1998).

I now turn to cointegration tests.

[6] The reason being that it is not clear why storms should depend on calendar time.

Table B.2 Simulated p-values for Stock and Watson's tests for the null of time-invariance against the alternative of random-walk time-variation in the mean of the first differences[a] of the series

	Radiative forcing:					Log	Sea		Temperature		
	anthropogenic[b]			volcanic[c]	solar	real	level	Storms	anomalies:		
HAC correction:	Mean	Median	Fraction below 10%			GDP			overall	land	ocean
	Trimming: 0.15										
Newey and West (1987)	0.0448	0.0148	0.8590	0.226	0.785	0.045	0.005	0.112	0.0004	0.000	0.049
Andrews (1991)	0.0531	0.0209	0.8590	0.348	0.874	0.063	0.008	0.071	0.0004	0.000	0.112
	Trimming: 0.25										
Newey and West (1987)	0.0409	0.0120	0.8480	0.892	0.784	0.027	0.006	0.195	0.0006	0.001	0.041
Andrews (1991)	0.0480	0.0171	0.8480	0.922	0.871	0.041	0.011	0.135	0.0006	0.000	0.088
	Trimming: 0.33										
Newey and West (1987)	0.0754	0.0488	0.7740	0.779	0.779	0.022	0.008	0.241	0.0004	0.003	0.044
Andrews (1991)	0.0864	0.0591	0.7700	0.813	0.854	0.032	0.014	0.184	0.0004	0.001	0.094

[a] For volcanic radiative forcing the level, controlling for the identified break in the mean.

[b] Mean and median of the Monte Carlo distribution of p-values, and fraction of p-values smaller than 10%.

B.3 Evidence from Wright's (2000) cointegration tests

I start from tests of cointegration between the JRF index and temperature anomalies. Based on the climate science literature, the relevant null hypothesis is that the level of the JRF index is cointegrated with the levels of temperature anomalies, so that even if all the series are I(2), the residual from the cointegrating regressions

$$T_t = a + bJRF_t + u_t, \tag{B.1}$$

where T_t is one of the temperature anomalies, is I(0). I therefore proceed as follows.

To fix ideas, let us focus on the land temperature anomaly. I start by generating, as previously described, 1,000 partially simulated series for the JRF index, JRF_t^j, with $j = 1$, 2, ..., 1,000. Then,

(1) based on each pair $\{JRF_t^j, T_t^{\text{Land}}\}$, $j = 1, 2, ..., 1{,}000$, I perform a Wright (2000) test for the null hypothesis of cointegration between JRF_t^j and T_t^{Land}. When the null is not rejected, this produces a confidence interval for the cointegration coefficient.

(2) Based on JRF_t^j, for $j = 1, 2, ..., 1{,}000$, and the other climate change series I estimate the model discussed in Section 4 in the main text. For each $j = 1, 2, ..., 1{,}000$, this produces $d = 1, 2, ..., 1{,}000$ draws from the posterior distribution of the estimated model.

(3) For each $j = 1, 2, ..., 1{,}000$, I then stochastically simulate each of the 1,000 d models (i.e. draws from the posterior), and based on these artificial data I perform the same test I performed in (1), thus building up a Monte Carlo distribution of Wright's (2000) test under the null hypothesis that the series are cointegrated in levels. In all cases in which the null is not rejected, this produces a corresponding confidence interval for the cointegration coefficient.

Evidence of cointegration is typically detected very strongly across the board between (*i*) the JRF index and the temperature anomaly; (*ii*) the level (not the logarithm) of real GDP and the first difference of anthropogenic RF; (*iii*) the temperature anomaly and either sea level or ice cover.

In particular, for either the land or the ocean temperature anomaly Wright's (2000) tests cannot reject the null hypothesis of cointegration for *any* $j = 1, 2, ..., 1{,}000$. Finally, as discussed in Section A.5 I integrate out the randomness associated with the simulated red noise I have added to the JRF index over the first part of the sample by computing the average, across all j's, of the confidence intervals for the cointegration coefficient.

The average across the 1,000 simulations of the 90%-coverage confidence interval for the cointegration coefficient for the land anomaly is [-0.95 -0.60], whereas the corresponding object for the ocean anomaly it is [-2.24 -1.45], reflecting the significantly slower rate of warming of the oceans over the sample period. It is to be noticed that the confidence intervals for the land and ocean anomalies are not overlapping. Taken at face value this would imply that the land and ocean anomalies, although both cointegrated with the JRF index, exhibit different long-run equilibrium relationships with it. Another possible interpretation is that, in response to a permanent increase in the JRF index, the two temperature anomalies ultimately increase by exactly the same amount, so that they share the same cointegration vector with the JRF, but that the sample period since 1850 is simply too short to capture this. As I discuss in the main text of the paper, climate science suggests that the former interpretation is significantly more plausible, and that in a long-run equi-

librium the land and the ocean exhibit different responses to a permanent increase in the JRF.

C Stock and Watson's (1996, 1998) Methodology for Searching for Random-Walk Time-Variation

In Appendix B.2 I test the null hypothesis of no time-variation in the mean of the first difference of climate change series against the alternative of random-walk time variation, based on Stock and Watson's (1996, 1998) TVP-MUB methodology applied to the AR(p) model

$$y_t = \mu + \phi_1 y_{t-1} + \phi_2 y_{t-2} + ... + \phi_p y_{t-p} + u_t = \theta' z_t + u_t \tag{C.1}$$

where y_t is the first difference of any of the series. I select the lag order, p, as the maximum among the lag orders selected by the Akaike and Schwartz information criteria, for a maximum possible number of lags P=20 years. In implementing the TVP-MUB methodology I closely follow Stock and Watson (1996, 1998). Letting θ_t=[μ_t, $\phi_{1,t}$, ..., $\phi_{p,t}$]$'$, the time-varying parameters version of (C.1) is given by:

$$y_t = \theta_t' z_t + u_t \tag{C.2}$$

$$\theta_t = \theta_{t-1} + \eta_t \tag{C.3}$$

with η_t *iid* $N(0_{p+1}, \lambda^2\sigma^2 Q)$, with 0_{p+1} being a (p+1)-dimensional vector of zeros; σ^2 being the variance of u_t; Q being a covariance matrix; and $E[\eta_t u_t]$=0. Following Nyblom (1989) and Stock and Watson (1996, 1998), I set Q=$[E(z_t z_t')]^{-1}$. Under such a normalisation, the coefficients on the transformed regressors, $[E(z_t z_t')]^{-1/2} z_t$, evolve according to a (p+1)-dimensional standard random walk, with λ^2 being the ratio between the variance of each 'transformed innovation' and the variance of u_t.[7]

The point of departure is the OLS estimate of θ in (C.1), $\hat{\theta}_{OLS}$. Conditional on $\hat{\theta}_{OLS}$ I compute the residuals, $\hat{u}_t$, and the estimate of the innovation variance, $\hat{\sigma}^2$, and I perform an *exp*-Wald test for a single break in the mean of y_t at an unknown point the sample as in (e.g.) Bai and Perron (1998, 2003) by regressing y_t on a constant, using either Newey and West's (1987) or Andrews' (1991) covariance matrix estimator to control for possible autocorrelation and/or heteroskedasticity in the residuals. I estimate the matrix Q as in Stock and Watson (1996) as

$$\hat{Q} = \left[T^{-1} \sum_{t=1}^{T} z_t z_t' \right]^{-1}.$$

I consider a 50-point grid of values for λ over the interval [0, 0.15], which I call Λ. For each $\lambda_j \in \Lambda$ I compute the corresponding estimate of the covariance matrix of η_t as $\hat{Q}_j$=$\lambda_j^2 \hat{\sigma}^2 \hat{Q}$, and conditional on $\hat{Q}_j$ I simulate model (C.2)-(C.3) 10,000 times as in Stock and Watson (1996, section 2.4), drawing the pseudo innovations from pseudo random *iid* $N(0, \hat{\sigma}^2)$. For each simulation, I compute an *exp*-Wald test (obviously, without however applying the

[7] To be precise, given that the Stock-Watson methodology is based on local-to-unity asymptotics, λ is actually equal to the ratio between τ, a small number which is fixed in each sample, and T, the sample length.

HAC correction) thus building up its empirical distribution conditional on λ_j. Based on the empirical distributions of the test statistic I then compute the median-unbiased estimate of λ as that particular value of λ_j which is closest to the statistic I previously computed based on the actual data. I compute the p-value based on the empirical distribution of the test conditional on λ_j=0. Finally, for reasons of robustness I consider three alternative values of trimming, 15, 25, and 33 per cent.

D The Metropolis-Within-Gibbs Estimation Algorithm

As mentioned in the main text, I estimate the model via Bayesian methods, based on a straightforward adaptation to the problem at hand of the Metropolis-within-Gibbs algorithm proposed by Justiniano and Primiceri (2008) to estimate DSGE models with stochastic volatility. Justiniano and Primiceri's (2008) algorithm (see their Appendix A) consisted of two 'blocks' of steps. In Block I the stochastic volatilities of the structural shocks, as well as their hyper-parameters, were drawn conditional on the parameters of the DSGE models via a Gibbs step. In Block II a Metropolis step was used in order to draw the DSGE model's parameters conditional on the stochastic volatilities. Within the present context in Block I the only difference with Justiniano and Primiceri (2008) is that I use a simpler specification for the stochastic volatilities. Instead of using their mixture of distributions, in line with e.g. Cogley and Sargent (2005) I postulate that any of the volatilities of the structural innovations evolves as in Jacquier, Polson, and Rossi (2002). As for Block II, instead of drawing the parameters of the DSGE models I obviously draw the parameters of the VAR, again via a Metropolis step.

D.1 Modelling the stochastic volatilities

Entering into details, the time-varying covariance matrix of the VAR's reduced-form innovations $u_t = A_0\epsilon_t$, where A_0 and ϵ_t are the same as in equation (9) in the main text, is factored as $\Omega_t = A_0 H_t A_0'$, where H_t is a diagonal matrix with the volatilities of the individual structural shocks ϵ_t on the diagonal, i.e.

$$H_t \equiv \begin{bmatrix} h_{1,t} & 0 & ... & 0 \\ 0 & h_{2,t} & ... & 0 \\ ... & ... & ... & ... \\ 0 & 0 & ... & h_{N,t} \end{bmatrix} \tag{D.1}$$

The $h_{i,t}$'s are postulated to evolve as geometric random walks, i.e.

$$\ln h_{i,t} = \ln h_{i,t-1} + \nu_{i,t} \tag{D.2}$$

For future reference, I define $h_t \equiv [h_{1,t}, h_{2,t}, ..., h_{N,t}]'$, $\nu_t \equiv [\nu_{1,t}, \nu_{2,t}, ..., \nu_{N,t}]'$, and $\beta \equiv [B_1, B_2, ..., B_p]$, where B_1, B_2, ..., B_p are the VAR matrices in equation (9) in the main text. I assume that $\epsilon_t \sim N(0, H_t)$ and $\nu_t \sim N(0, Z)$, with

$$Z = \begin{bmatrix} \sigma_1^2 & 0 & ... & 0 \\ 0 & \sigma_2^2 & ... & 0 \\ ... & ... & ... & ... \\ 0 & 0 & ... & \sigma_N^2 \end{bmatrix} \tag{D.3}$$

Finally, I assume that ϵ_t and ν_t are orthogonal both contemporaneously, and at all leads and lags.

D.2 Priors

The prior distribution for the initial values of the stochastic volatilities, the h_0's, is postulated to be normal, and it is assumed to be independent from the distribution of the hyperparameters. I calibrate the prior distribution for h_0 as

$$\ln h_{i,0} \sim N(-5, 10) \tag{D.4}$$

The large variance, 10, insures that the prior is very weakly informative. Finally, for the variances of the stochastic volatility innovations I follow Cogley and Sargent (2005) and I postulate an inverse-Gamma distribution for the elements of Z,

$$\sigma_i^2 \sim IG\left(\frac{10^{-4}}{2}, \frac{1}{2}\right) \tag{D.5}$$

D.3 Simulating the posterior distribution

Conditional on the data, I simulate the posterior distribution of the VAR parameters, the hyperparameters, and the stochastic volatilities *via* the following Metropolis-within-Gibbs algorithm. In what follows, x^t denotes the entire history of the vector x up to time t—i.e. $x^t \equiv [x_1', x_2', \quad , x_t']'$—while T is the sample length. At iteration i the algorithm proceeds as follows:

(a) drawing the elements of H_t Conditional on Y^T (i.e., the entire data sample) and the VAR's parameters β, the structural shocks $\epsilon_t = A_0^{-1} u_t$, where u_t are the VAR's reduced-form residuals, with Var(ϵ_t)=H_t, are observable. Following (Cogley and Sargent, 2005), I then sample the $h_{i,t}$'s by applying the univariate algorithm of Jacquier, Polson, and Rossi (2004) element by element.[8]

(b) Drawing the hyperparameters Conditional on Y^T, β, and $h_{i,t}$'s, the innovations to the $h_{i,t}$'s are observable, which allows to draw the hyperparameters (i.e. the σ_i^2) from their respective distributions.

(c) Drawing the VAR's parameters Conditional on Y^T and the $h_{i,t}$'s, I draw the VAR's parameters via a Metropolis step. Specifically, a new candidate parameter β^* is drawn from a proposal density based on the likelihood of the VAR's parameters conditional on the data and the stochastic volatilities drawn in step (a). The candidate draw is accepted with probability

$$r = \min\left[1; \frac{L(Y^T|\beta^*, H_i^T)\pi(\beta^*)}{L(Y^T|\beta_{i-1}, H_i^T)\pi(\beta_{i-1})}\right] \tag{D.6}$$

where $L(Y^T|\beta_{i-1}, H_i^T)$ is the likelihood of the data conditional on (1) the VAR's parameters' draw at iteration i-1 (i.e., β_{i-1}), and (2) the stochastic volatilities at iteration i previously drawn in nstep (a); $L(Y^T|\beta^*, H_i^T)$ is the corresponding likelihood of the data conditional on the candidate draw β^*, instead pf β_{i-1}; and $\pi(\beta^*)$ and $\pi(\beta_{i-1})$ are the prior densities of β^* and β_{i-1}.

[8] In fact I use Cogley and Sargent's (2005) MATLAB codes, which were kindly provided by Tim Cogley.

Conditional on the data, the algorithm simulates the posterior distribution of the VAR parameters, the hyperparameters, and the stochastic volatilities by iterating on (a)-(c).

I run a burn-in pre-sample of 1,000,000 draws which I then discard. I then generate 10,000,000 draws, which I 'thin' by sampling every 1,000 draws in order to reduce their autocorrelation. This leaves 10,000 draws from the ergodic distribution which I use for inference. For all models the fraction of accepted draws is very close to the ideal one, in high dimensions, of 0.23 (see Gelman, Carlin, Stern, and Rubin, 1995). I check convergence of the Markov chain based on Geweke's (1992) inefficiency factors (IFs) of the draws from the ergodic distribution for each individual parameter. For all parameters the IFs are equal to at most 3-4, well below the values of 20-25 which are typically taken to indicate problems in the convergence of the Markov chain.

E References

Andrews, D.W.K. (1991): "Heteroskedasticity and Autocorrelation-Consistent Covariance Matrix Estimation", *Econometrica*, 59(3), 817-858.

Bai, J. and P. Perron (1998): "Estimating and Testing Linear Models with Multiple Structural Changes", *Econometrica*, 66(1), 47-78

Bai, J. and P. Perron (2003): "Computation and Analysis of Multiple Structural Change Models", *Journal of Applied Econometrics*, 18(1), 1-22

Benati, L. (2007): "Drift and Breaks in Labor Productivity", *Journal of Economic Dynamics and Control*, 31, 2847-2877.

Butler, J.H., and Montzka, S.A. (2018): "The NOAA Annual Greenhouse Gas Index (AGGI)", NOAA Earth System Research Laboratory, Boulder, CO

Christiano, L. J., and T. J. Fitzgerald (2003): "The Bandpass Filter", *International Economic Review*, 44(2), 435-465.

Church, J.A., and White, N.J. (2006): "A 20th century acceleration in global sea-level rise", *Geophysical Research Letters*, 33, L01602.

Coddington, O., Lean, J.L., Pilewskie, P., Snow, M., Lindholm, D. (2015): "A Solar Irradiance Climate Data Record", *Bulletin of the American Meteorological Society*, p. 1265-1282.

Crowley, T.J. and M.B. Unterman (2012): "Technical details concerning development of a 1200-yr proxy index for global volcanism", *Earth System Science Data*, Vol. 5, pp. 187-197.

Dergiades, T., Kaufmann, R.K., Panagiotidis, T. (2016): "Long-Run Changes in Radiative Forcing and Surface Temperature: The Effect of Human Activity Over the Last Five Centuries", *Journal of Environmental Economics and Management*, 76, 67-85.

Diebold, F.X. and Chen, C. (1996): "Testing Structural Stability with Endogenous Breakpoint: A Size Comparison of Analytic and Bootstrap Procedures", *Journal of Econometrics*, 70(1), 221-241.

Elliot, G., T.J. Rothenberg and J.H. Stock (1996): "Efficient Tests for an Autoregressive Unit Root", *Econometrica*, 64(4), 813-836.

Justiniano, A. and Primiceri, G.E. (2008): "The Time-Varying Volatility of Macroeconomic Fluctuations", *American Economic Review*, 98:3, 604-641.

Kaufmann, R.K. and D.I. Stern (2002), "Cointegration Analysis of Hemispheric Temperature Relations", *Journal of Geophysical Research*, Vol. 107, N. D2, 4012, 10.1029/2000JD000174.

Kaufmann, R.K., H. Kauppi, and J.H. Stock (2006): "Emissions, Concentrations, and Temperature: A Time Series Analysis", *Climatic Change*, 77: 249-278.

Kaufmann, R.K., H. Kauppi, and J.H. Stock (2010): "Does Temperature Contain a Stochastic Trend? Evaluating Conflicting Statistical Results", *Climatic Change*, 101:395-405.

Kaufmann, R.K., H. Kauppi, M.L. Manna, and J.H. Stock (2011), "Reconciling Anthropogenic Climate Change with Observed Temperature 1998–2008, PNAS, July 19, 2011, Vol. 108, n. 29.

Koop, G., Strachan, R., van Dijk, H., and Villani,M. (2006): "Bayesian Approaches to Cointegration", in K. Patterson and T. Mills, editors, *The Palgrave Handbook of Theoretical Econometrics*, Palgrave MacMillan

Koop, G., Léon-González, R., and Strachan, R.W. (2010): "Efficient Posterior Simulation for Cointegrated Models with Priors on the Cointegration Space", *Econometric Reviews*, 29(2), 224-242

Kopp, G. and G. Lawrence (2005): "The Total Irradiance Monitor (TIM): Instrument Design", *Solar Physics*, 230(1), 91-109.

Kopp, G, K. Heuerman, and G. Lawrence (2005): "The Total Irradiance Monitor (TIM): Instrument Calibration", *Solar Physics*, 230(1), 111-127.

Kopp, G., Krivova, N., Lean, J., and C.J. Wu (2016): "The Impact of the Revised Sunspot Record on Solar Irradiance Reconstructions", *Solar Physics*, p. 1-18.

Newey, W. and K. West (1987): "A Simple Positive-Semi-Definite Heteroscedasticity and Autocorrelation Consistent Covariance Matrix", *Econometrica*, 55, 703-708.

Nyblom, J. (1989), "Testing for the Constancy of Parameters Over Time", *Journal of the American Statistical Association*, 84(405), 223-230.

Robertson, A., Overpeck, J., Rind, D., Mosley-Thompson, E., Zielinski, G., Lean, J., Koch, D., Penner, J., Tegen, I., and Healy, R. (2001): "Hypothesized Climate Forcing Time Series for the Last 500 Years", *Journal of Geophysical Resesearch Atmosphere*, Vol. 106(D14), p. 14, 783.

Schallock, J., Brühl, C., Bingen, C., Höpfner, M., Rieger, L., and Lelieveld, J. (2023): "Reconstructing volcanic radiative forcing since 1990, using a comprehensive emission inventory and spatially resolved sulfur injections from satellite data in a chemistry-climate model", *Atmospheric Chemistry and Physics*, 23, 1169-1207.

Shine, K.P.R.G., Derwent, D.J., Wuebbles, D.J., and Mocrette, J.J. (1991): "Radiative Forcing of Climate", in Houghton, J.T., Jenkins, G.J., and Ephramus, J.J., editors, *Climate Change: The IPCC Scientific Assessment*, Cambridge University Press, Cambridge, pp. 47-68.

Stern, D.I. and Kaufmann, R.K. (2000): "Detecting a Global Warming Signal in Hemispheric Temperature Series: A Structural Time Series Analysis", *Climatic Change*, 47, 411-438.

Stern, D.I. and Kaufmann, R.K. (2014): "Anthropogenic and Natural Causes of Climate Change", *Climate Change*, 122, 257-269.

Stock, J. and Watson, M. (1996): "Evidence of Structural Instability in Macroeconomic Time Series Relations", *Journal of Business and Economic Statistics*, 14(1), 11-30.

Stock, J. and Watson, M. (1998): "Median-Unbiased Estimation of Coefficient Variance in a Time-Varying Parameter Model", *Journal of the Americal Statistical Association*, 93(441), 349-358.

Walsh, J. E., W. L. Chapman, F. Fetterer, and S. Stewart (2019): "Gridded monthly sea ice extent and concentration, 1850 onward, version 2", NSIDC: National Snow and Ice Data Center, Boulder, Colorado USA.

Wright, J.H. (2000): "Confidence Sets for Cointegrating Coefficients Based on Stationarity Tests", *Journal of Business and Economic Statistics*, 18(2), 211-222.